2017

Lysin Based Antimicrobial Peptides Against Acinetobacter Baumannii

Mya Thandar

LYSIN BASED ANTIMICROBIAL PEPTIDES AGAINST *ACINETOBACTER BAUMANNII*

A Thesis Presented to the Faculty of

The Rockefeller University

in Partial Fulfillment of the Requirements for

the degree of Doctor of Philosophy

by

Mya Thandar

June 2017

LYSIN BASED ANTIMICROBIAL PEPTIDES AGAINST *ACINETOBACTER BAUMANNII*

Mya Thandar, Ph.D.
The Rockefeller University 2017

Acinetobacter baumannii is a Gram-negative bacterial pathogen responsible for a range of nosocomial infections. The recent rise and spread of multidrug resistant *A. baumannii* clones has fueled a search for alternative therapies, including bacteriophage endolysins with potent antibacterial activities. A common feature of these lysins is the presence of a highly positively charged C-terminal domain with a likely role in promoting outer membrane penetration. In the current study, we show that the C-terminal amino acids 108-138 of phage lysin PlyF307, named P307, alone was sufficient to kill *A. baumannii* (>3-logs). Furthermore, P307 could be engineered for improved activity, the most active derivative being $P307_{SQ-8C}$ (>5-log kill). Both P307 and $P307_{SQ-8C}$ showed high *in vitro* activity against *A. baumannii* in biofilms. Moreover, $P307_{SQ-8C}$ exhibited MICs comparable to levofloxacin and ceftazidime and acted synergistically with polymyxin B. While the peptides were shown to kill by disrupting the bacterial cytoplasmic membrane, they did not lyse human red blood cells or B cells; however, serum was found to be inhibitory to lytic activity. In a murine model of *A. baumannii* skin infection, $P307_{SQ-8C}$ reduced the bacterial burden by ~2-logs in 2 h. This study demonstrates the prospect of using peptide derivatives from bacteriophage lysins to treat topical infections and remove biofilms caused by Gram-negative pathogens.

To my grandparents

To my parents

To Neko

ACKNOWLEDGMENTS

Foremost, I would like to thank Dr. Vincent Fischetti for being the most understanding and supportive mentor. Words could not express my gratitude to him. He has always been available for discussing my work and each discussion has challenged and cultivated me to become a better scientific thinker. Throughout my graduate studies, his wisdom has guided me and his encouragement has motivated me. It has been a privilege having him as my advisor and mentor.

I am grateful to my faculty advisory committee: Dr. Luciano Marraffini and Dr. Howard Hang. Their insights and counsels have been stimulating and invaluable for my progress. I would also like to thank Dr. Ryland Young for kindly accepting a position on my committee as the external examiner.

I am thankful to Dr. Rolf Lood and Benjamin Winer for showing me the ropes in the lab. They have played crucial roles in helping me launch my thesis project. Dr. Chad Euler has patiently guided and assisted me in conducting *in vivo* experiments. I am also grateful to Clara Eastby and my summer students Ravenne Reid and Gabriella Balaa for their excellent assistance. I am much obliged to the past and present members of the Fischetti Laboratory who have contributed to my project by providing valuable feedbacks and ideas. Thanks to the cordial and collaborative space they provided, this journey has been an enjoyable one. I also want to thank Dr. Michael Wittekind and Dr. Raymond Schuch for their useful discussions and suggestions and ContraFect Corporation for the funding support.

I am incredibly grateful to the Rockefeller community for providing the ideal place to hone my scientific skills. The Proteomics Resource Center, the Electron

Microscopy Resource Center, the Comparative Bioscience Center and the Hospital have contributed their technical expertise to my research. The Housing and Security Departments and the mailroom have ensured my safe and comfortable living environment. Everyone in the Dean's Office – Dr. Sidney Strickland, Dr. Emily Harms, Dr. Andrea Morris, Marta Delgado, Kristen Cullen, Cris Rosario and Stephanie Fernandez – have enabled me to fulfill my academic aspirations without an issue.

I would like to thank my past mentors Dr. Seth Darst, Dr. Joseph Osmundson, Dr. Lilian Hsu and Tenaya Vallery who have shared with me the joy of scientific discovery. Lastly, I would like to thank all my friends and family who have sustained me with their unwavering love and kindness.

TABLE OF CONTENTS

LIST OF FIGURES

LIST OF TABLES

1 CHAPTER 1 – INTRODUCTION

1.1 *Acinetobacter baumannii*

Acinetobacter baumannii is a strictly aerobic Gram-negative bacterium and belongs to the family *Moraxellaceae*. As an opportunistic pathogen, it causes hospital-acquired or nosocomial infections worldwide (1). The treatment options are greatly limited by its intrinsic and acquired resistance to all classes of antibiotics (2, 3).

1.1.1 History

The designation of *A. baumannii* has changed a great deal over time. When first reported by Beijerinck in 1911, *A. baumannii* was characterized as a soil bacterium and was called *Micrococcus calcoaceticus* (4, 5). Only in the 1950s did it acquire its current genus identification *Acinetobacter* after being known under various genera, such as *Achromobacter anitratus*, *Moraxella lwoffii*, *Neisseria winogradskyi*, to name just a few. Current nomenclature, suggested by Brisou and Prevot in 1954, stemmed from the bacterium's non-motile phenotype (akinetos meaning non-motile in Greek) and was officially recorded with a single species *A. calcoaceticus* in Bergey's Manual of Systematic Bacteriology in 1974 (6, 7). Presently the *Acinetobacter* genus contains over 50 species among which *A. baumannii*, *A. calcoaceticus*, *A. haemolyticus*, *A. nosocomialis* and *A. pittii* are of high clinical relevance and *A. baumannii* is the most prominent with highest morbidity and mortality rate (6-8).

Not only has the nomenclature evolved but the antibiotic susceptibility has also changed over the last century for *A. baumannii*. During the 1960s and early 70s, nosocomial infections by *Acinetobacter* had already been reported in Europe and the United States despite limited methods for pathogen identification. The etiologic agents of

these outbreaks, still called *Acinetobacter anitratus*, were of low pathogenicity and could be easily controlled by β-lactams, sulfonamides and aminoglycosides (9). However, beginning in late 70s, 80s and 90s, these antibiotics had progressively become ineffective and multidrug-resistant clones emerged worldwide (10, 11). In addition, advances in molecular techniques during these decades enabled the identification of *baumannii* species as the cause of the majority of *Acinetobacter* infections (6). In the 2000s and 2010s, problems with antibiotic-resistant *A. baumannii* worsened resulting in the establishment of surveillance networks worldwide to increase awareness and better containment (6). Notably in 2006, The Infectious Diseases Society of America included *A. baumannii* in the list of ESKAPE pathogens (*Enterococcus faecium*, *Staphylococcus aureus*, *Klebsiella pneumoniae*, *A. baumannii*, *Pseudomonas aeruginosa* and *Enterobacter* spp.) for which only limited treatment options were available (12). Moreover, in February 2017, the World Health Organization (WHO) emphasized the urgent need for new drugs against this pathogen by listing *Acinetobacter* in the most critical category on which research and development (R&D) efforts for new antibiotics should be focused (13). *A. baumannii* has risen from a harmless bacterium to one of the most clinically severe pathogens in the past century (Figure 1.1). To stay ahead of this pathogen, diverse strategies must be concurrently employed, including but not limited to prevention and control, antibiotic stewardship, as well as novel therapeutic development.

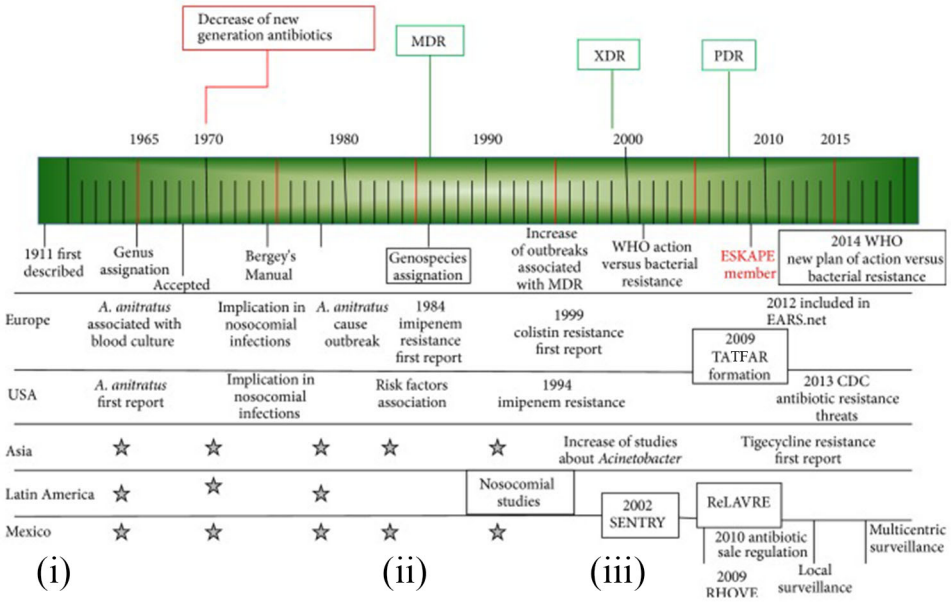

MDR – multidrug resistant; XDR – extensively drug resistant; PDR – pandrug resistant; TATFAR – Transatlantic Taskforce on Antimicrobial Resistance; CDC - Center of Disease Control and Prevention; SENTRY, ReLAVRE and RHOVE – antimicrobial surveillance program

Figure 1.1 Significant events in the history of *A. baumannii*.

The timeline consists of three milestones, (i) awareness and diagnosis, (ii) rise of antibiotic resistance, and (iii) resistance containment and surveillance efforts by international organizations. Adapted by permission (Creative Commons Attribution License) from Hindawi Publishing Corporation: Journal of Pathogens (6), copyright 2016.

1.1.2 Prevalence and pathogenesis

A. baumannii is an increasingly significant opportunistic pathogen worldwide (2). Its natural habitats are soil and water. In healthy children and immuno-compromised adults, it can cause community-acquired respiratory tract infections (7). Community-acquired pneumonia is currently limited to the tropical regions of the world and occurs during warm and humid months (14). However, nosocomial infections are prevailing in healthcare facilities worldwide. The important reservoirs in hospital outbreaks are patients, healthcare workers and equipment (15). *A. baumannii* also persists for long periods on abiotic surfaces under dry conditions (16). From contaminated indwelling devices, surgical equipment and ventilators, *A. baumannii* can infect various body sites (Figure 1.2) and cause meningitis, keratitis, opthalmitis, wound, respiratory and urinary tract infections, pneumonia and bacteremia (17). According to the CDC report in 2013, 7,300 clinical isolates out of 12,000 *Acinetobacter* cases were multi-drug resistant (untreatable by three or more antibiotic categories) and 500 deaths were attributed to those infections annually in the United States alone (18). Given the widespread prevalence and severe pathogenesis, it is essential to develop new strategies to control *A. baumannii* in healthcare settings.

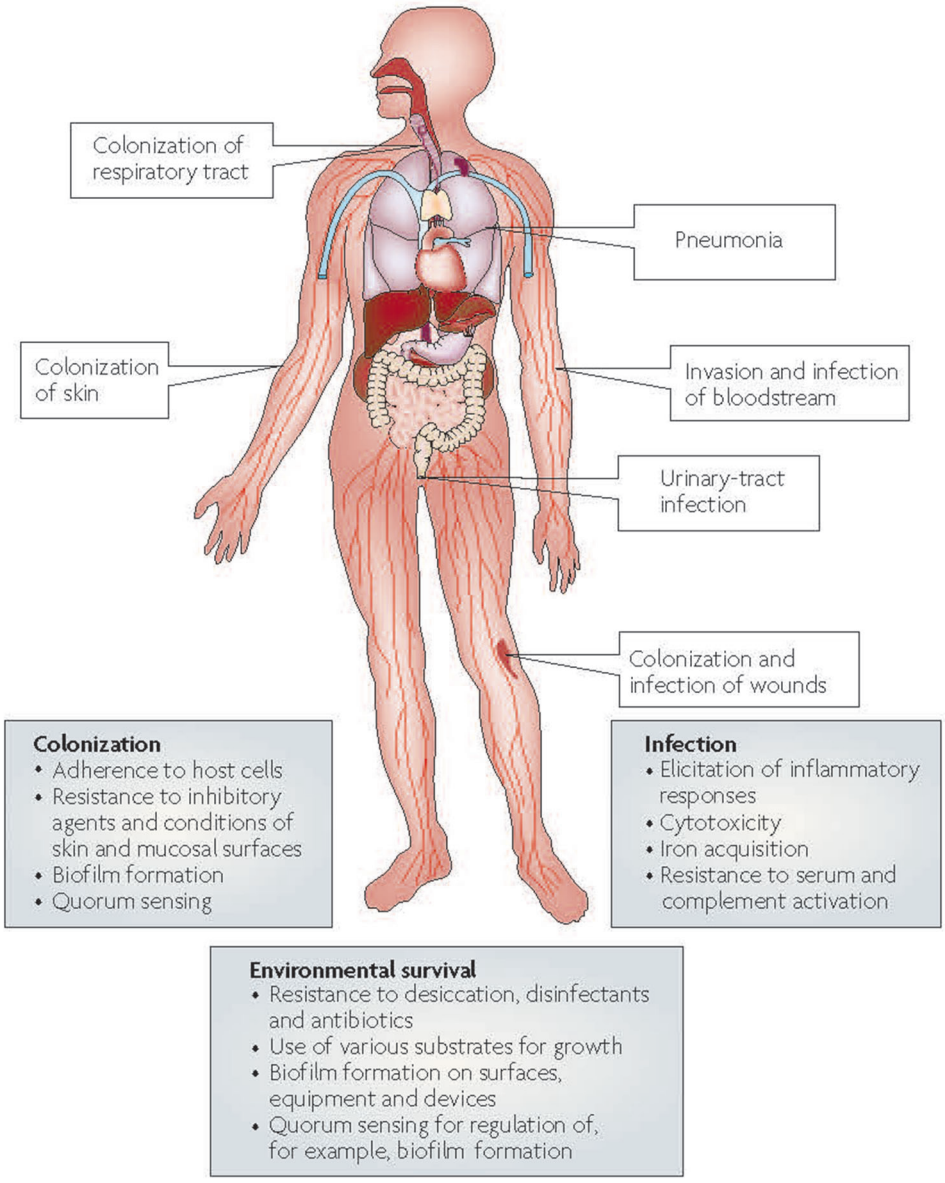

Figure 1.2 Pathogenesis and virulence of *A. baumannii*.

A. baumannii colonizes different parts of the body and causes infections when opportunities arise (e.g. weakened immune system, skin lesions, etc.) The pathogen has high tolerance to environmental stress, creating inanimate reservoirs in healthcare settings. With its varied virulence factors and antibiotic resistance, *A. baumannii* is indeed a formidable foe in hospitals. Reprinted by permission from Macmillan Publishers Limited: Nature Reviews Microbiology (17), copyright 2007.

1.1.3 Virulence and antibiotic resistance

A. baumannii employs several virulence factors to compromise host cells and evade immune system (Figure 1.2). The factors include outer membrane proteins (Omp), secretion systems, toxins, iron-chelating siderophores, capsule and lipopolysaccharide (LPS). Like other Gram-negative bacteria, *A. baumannii* utilizes Omp for adherence, invasion and cytotoxicity, e.g. OmpA has been shown to be essential for epithelial cell binding and for producing outer membrane vesicles that deliver virulence factors to human host cells (19-22). The Type II secretion system is used to secrete lipases, proteases and toxins that are important for *in vivo* fitness and pathogenesis (23). After invasion, *A. baumannii* survives in iron-limiting host environments by utilizing siderophores (24). Last, but not least, *A. baumannii* achieves serum resistance, eludes complement, neutrophils and antibodies by capsule (25) and modified LPS (26).

Besides the virulence factors, *A. baumannii* possesses assorted mechanisms of antibiotic resistance (27). Being naturally competent, the pathogen is capable of taking up environmental DNA for increased survival advantages (28). Other modes of horizontal gene transfer such as plasmid conjugation and bacteriophage transduction have resulted in the expansion of its chromosomal repertoire for drug resistance (7). The intrinsic and acquired resistance mechanisms (Table 1.1) include low permeability that limits antibiotic uptake, efflux pumps that decrease intracellular antibiotic concentration, biofilm formation that restricts metabolism to attenuate antibiotic effect, antibiotic target site mutations and antibiotic-deactivating enzymes (27). As a result, most of *A. baumannii* clinical isolates these days are either multi-drug resistant (MDR) or extensively drug resistant (XDR or susceptible to only one or two classes of antibiotics) or pan-drug resistant (PDR or resistant to all antibiotics).

1.1.4 Treatment

A. baumannii has successfully overcome most of the clinically approved antibiotics with one or more of the resistance mechanisms mentioned above. As such, the treatment options are limited. The antibiotics for *A. baumannii* infections have traditionally been cephalosporins, sulbactam, carbepenems, rifampin, fluoroquinolones, aminoglycosides, tetracyclines and polymyxins (Table 1.1). The first three classes, being of β-lactam family, target the peptidoglycan synthesis and *A. baumannii* neutralizes them by class A-D β-lactamases and penicillin-binding proteins (PBPs). To counteract rifampin, fluoroquinolones and aminoglycosides, *A. baumannii* strains with mutations in the drug binding sites of RNA polymerase, DNA topoisomerase and ribosome respectively have arisen. Tetracyclines, protein synthesis inhibitors, are blocked by Tet proteins that bind to 70S ribosome for protection. Polymyxins kill *A. baumannii* by interacting with LPS through positively charged Dab (α,γ-diaminobutyric acid) residues and destabilizing the outer membrane. Even the drugs of last resort, polymyxins are marred with suboptimal pharmacokinetics and safety issues as well as resistance by LPS modification. Currently, PDR *A. baumannii* infections are treated with combination therapy, i.e. two or more drugs that are shown to have *in vitro* synergy (e.g. colistin and rifampin). However, clinical trial data relevant to the efficacy of mono therapy vs. combination therapy are limited since most of the latter have so far been salvage options for severe cases (29). In view of the lack of novel antibiotic class to treat *A. baumannii* and the increasing threat of drug resistance, alternative strategies such as phage-based therapy must be considered and analyzed to fill the unmet need.

Table 1.1 Antibiotics versus *A. baumannii* (29)

Classes of antibiotics	**Targets**	**Resistance mechanisms**
Cephalosporins	Cell wall synthesis	*Acinetobacter*-derived cephalosprinase (ADC), extended spectrum β-lactamases (ESBL)
Carbepenems	Cell wall synthesis	Carbepenamases (OXA-groups, metallo-β-lactamases), reduced permeability, active efflux
Sulbactam	β-lactamases or PBPs	Reduced expression of the targets
Rifampin	RNA polymerase	RNA polymerase modification, rifampin modifying enzyme, active efflux
Aminoglycosides	16S ribosomal RNA (protein synthesis)	16S ribosomal RNA modification, aminoglycoside modifying enzymes
Fluoroquinolones	DNA gyrase and topoisomerase	Modifications in the quinolone resistance determining region, active efflux
Colistin	LPS	LPS modification or loss
Tetracyclines	30S ribosomal RNA (protein synthesis)	Ribosomal protection proteins, active efflux

1.2 Alternative antibacterial agents

1.2.1 Bacteriophages

The interest in bacteriophage therapy has been rekindled by the rise of drug-resistant bacteria together with the lack of new antibiotics in the R&D pipeline (30). The discovery and characterization of phages in 1917 and the subsequent demonstration of their therapeutic potential predated the beginning of antibiotic era by 11 years. However, after the industrialization of penicillin and subsequent drugs, only the former Soviet Union and Eastern Europe continued to pursue phage studies and use phage cocktails to treat bacterial infections. The rest of the world had switched away from phage therapeutics to antibiotics for a number of reasons: efficacy, safety, resistance, manufacturing (31). Now, with the imminent possibility that we may be entering a post-antibiotic era, western research institutions and government agencies are re-considering this century-old biological approach to kill bacteria (32, 33).

Before phages can be introduced to clinics in the western world, barriers must be overcome to obtain regulatory approval (34). A few of the hurdles originate from the nature of phage reproduction. Phages, as viruses of bacteria, can adopt lysogenic or lytic life cycles to multiply. After injecting their DNA into bacteria, temperate phages can display lysogenic cycle and replicate along as prophages until environmental cues induce them to enter a lytic cycle. On the other hand, virulent phages display lytic cycle only and assemble phage progeny using cellular machineries of bacteria. The lytic cycle culminates in bacterial lysis and release of phages to infect neighboring bacteria (Figure 1.3). Therefore, lytic phages, regardless of being virulent or temperate, could theoretically multiply at the site of application and lower the bacterial burden to control

infections. However, the use of temperate phages can spread antibiotic resistance genes since phages can act as carriers of genetic materials among bacteria. Another safety concern is the activation of detrimental inflammatory responses to the released bacterial components (and endotoxins in the case of Gram-negative bacteria) by massive bacterial lysis. In addition, phages are often strain-specific and phage cocktails are required to cover a single species of pathogen. On the flip side, the specificity can sometimes limit the unintended killing of commensal microflora. Like antibiotics, phage cocktails can become ineffective as bacteria develop resistance. Therefore the treatments must be monitored and modified. Phage resistance, however, is more easily tackled than antibiotic resistance due to the tremendous diversity of phages for some species in nature resulting from the arms race between phages and bacteria through hundreds of millions of years. Unfortunately, the diversity could mean more regulatory requirements (31, 34). For these reasons and others, phages have yet to appear in western clinics.

Despite the barriers and challenges, a number of strategies are in place to bring the phages from bench to bedside. One such approach is genetically engineering phages for different purposes. Some engineering tactics include creating: phages with reduced lysis to mitigate inflammatory responses; phages that increase antibiotic susceptibility of bacteria; phages that target pathogens with DNA sequence specificity, e.g. antibiotic resistance genes; phages with broader host ranges and so forth (35). Along with these creative scientific efforts, more clinical data are required to acquire regulatory approval. Although the long-established use of phage therapy in Russia, Poland and Georgia should have warranted the efficacy and safety, those clinical trials were not conducted with appropriate controls, and so the Eastern European experience has not provided any useful

proof of efficacy by Western standards. To fill this knowledge gap, the Phagoburn clinical trial, funded by European Commission, is in progress to access the efficacy and safety of phages in treating burn wounds infected by *Escherichia coli* or *Pseudomonas aeruginosa* (ClinicalTrials.gov Identifier NCT02116010). The results from all the scientific and clinical endeavors may pave the way for phages towards clinical use.

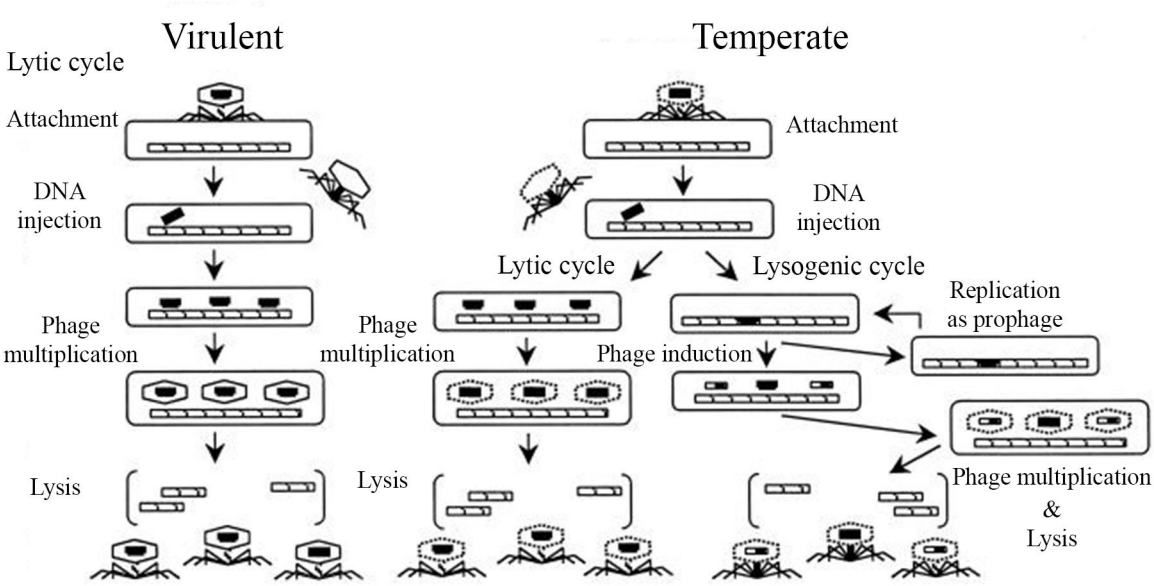

Figure 1.3 Life cycles of virulent and temperate phages.

After phage attachment and DNA injection into host bacteria, virulent phages display lytic cycle whereas temperate phages can enter either lytic or lysogenic cycle. During the lytic cycle, phages multiply inside bacteria and the fate of the host is lysis. On the other hand, phages replicate along with host bacteria as prophages during the lysogenic cycle. The host bacteria or lysogens survive until prophages re-enter lytic cycle by environment cues (e.g. UV damage to DNA). As phages multiply, they can package bacterial DNA and bring about transduction or phage-mediated horizontal gene transfer among bacteria. Adapted by permission from American Society for Microbiology: Antimicrobial Agents and Chemotherapy (31), copyright 2001.

1.2.2 Phage lysins

Just as bacterial defenses against antibiotics are multipronged, the development of ammunition against bacterial pathogens must progress in a multifaceted fashion. The regulatory bottleneck for phages has prompted innovations in bactericidal phage products such as endolysins (lysins). These are enzymes used by phages to degrade the bacterial cell wall for lysis at the end of the lytic cycle. They are classified as peptidoglycan hydrolases and lyases that cleave a variety of bonds in the bacterial peptidoglycan (36). With few exceptions such as PlySs2 that kills both *Streptococcus suis* and *Staphylococcus aureus* (37), the target bacteria of each lysin fall within a single genus or species. Recombinant lysins against Gram-positive bacteria have been shown to be effective bactericidal agents that cause hypotonic lysis (e.g. PlyC against *Streptococcus* spp. (38), PlyG against *Bacillus anthracis* (39), etc.) Typically, each lysin is made up of one or two N-terminal catalytic domains (CD) and a C-terminal cell wall binding domain (CWBD) (40), with the notable exception of PlyC, a multimeric enzyme comprised of a catalytic PlyCA subunit and a binding PlyCB octamer) (38). Compared to phages, lysins present fewer regulatory challenges since cocktails are unnecessary and there is virtually no concern for resistance development or spread of antibiotic resistance genes. The immunogenicity of lysins is also negligible but inflammatory responses could be triggered by dead bacterial components. Overall, lysins are promising antimicrobials against Gram-positive bacteria (40).

In contrast, the Gram-negative counterparts are relatively less active because the outer membrane largely limits the accessibility of subjacent peptidoglycan (Figure 1.4). Different strategies have been employed to increase the membrane permeability to lysins,

including the use of the chelating agent EDTA (41, 42), and the modification of lysins with either highly charged/hydrophobic N-/C-terminal extensions (43) or other membrane translocating domains (44, 45). The success of each approach varies in terms of efficacy increase and clinical applicability.

Nonetheless, a few naturally active lysins have been identified and characterized, e.g. LysAB2 (46) and PlyF307 (47). LysAB2 was isolated from lytic phage ΦAB2 and was shown to have bactericidal activities against *Streptococcus sanguis*, *A. baumannii* and *E. coli* (46). On the other hand, PlyF307 was identified as the most active lysin among those isolated by screening for inducible lysis genes cloned from a genomic library of prophages from 13 *A. baumannii* strains. It was shown to be specifically active against *A. baumannii* and to be able to rescue mice from lethal bacteremia (47). These lysins are capable of killing *A. baumannii* in spite of the outer membrane barrier. Both LysAB2 and PlyF307 employ distinct domain structures. Instead of the conventional CD-CWBD motif, they are composed of an N-terminal lysozyme-like domain and a C-terminal positively charged peptide (Figure 1.5). The C-terminus of LysAB2 putatively forms an amphipathic helix and without it, LysAB2 was shown to lose 40% of its bactericidal activity. It has also hypothesized that the positively charged peptide promotes the membrane trespassing (46). This project focuses on the characterization of such a peptide from PlyF307 as an antimicrobial peptide against *A. baumannii*.

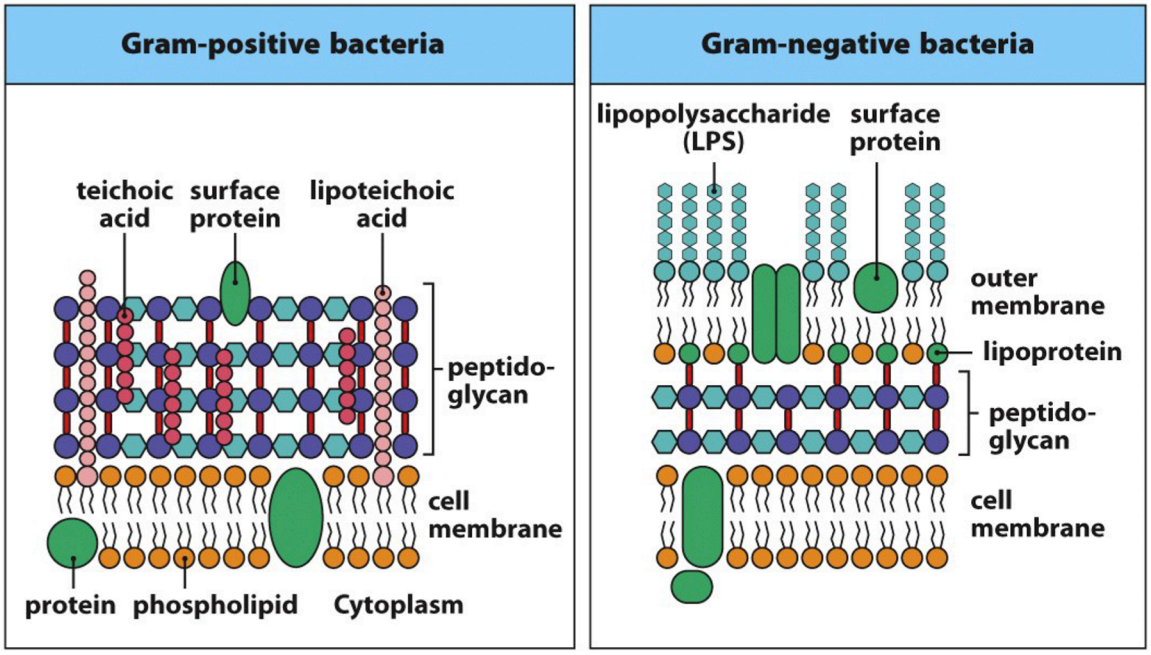

Figure 1.4 Simplified cell wall structures of Gram-positive and Gram-negative bacteria.

Recombinant phage lysins can effectively cleave the exposed peptidoglycan and bring about hypotonic lysis in Gram-positive bacteria. In contrast, Gram-negative phage lysins have only limited access to their peptidoglycan substrate because of the outer membrane. Adapted by permission from Taylor andFrancis Group: Janeway's Immunobiology, 8th Edition (48), copyright Garland Science 2012.

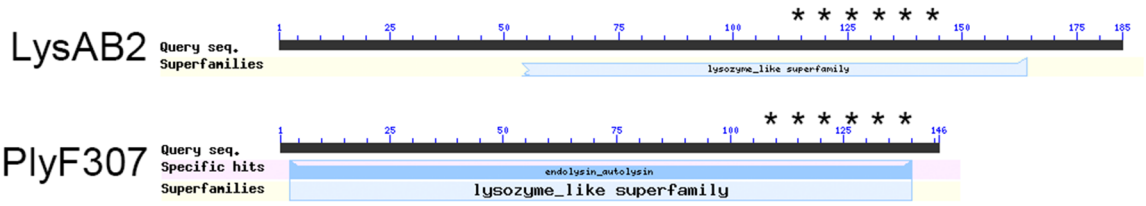

Figure 1.5 Putative conserved domains of LysAB2 and PlyF307.

According to a National Center for Biotechnology Information Basic Local Alignment Search Tool (BLAST) search, both LysAB2 and PlyF307 contain lysozyme-like domains. The stars (*) mark the putative amphipathic helix (46) in LysAB2 (amino acids 113-145) and the similar region with a high positive charge (+7) in PlyF307 (amino acids 108-138).

1.2.3 Antimicrobial peptides

Antimicrobial peptides (AMPs) represent an important class of weapons in the fight against bacteria. They are ubiquitous in all living organisms and come in different sequences and structures, e.g. cationic LL-37 human cathelicidin with an amphipathic α-helix (49), cysteine-rich pig protegrin-1 with anti-parallel β-strands (50), anionic human dermcidin with α-helix that forms hexameric bundle (51), antimicrobial peptide from human hepatitis B virus core protein arginine-rich domain (HBc ARD) (52) and so on. Like antibiotics, they have varied mechanisms of action, but primarily kill by permeabilizing the membrane. While they show great potential for clinical use, AMPs also present several safety concerns including toxicity and resistance development. Membrane permeabilization by AMPs is usually concentration dependent. Although mammalian membranes are spared because of the differences in lipid compositions, the selectivity could be nullified at higher doses (53). Similarly, the likelihood is low for bacteria to become resistant to AMPs. However, the immune evasion by pathogens could be exacerbated if bacteria do develop resistance that is cross reactive to human AMPs, a crucial part of innate immunity (54). Even with these safety concerns, a few AMPs are in clinical trials for topical applications (53), indicating that AMPs are viable options to combat antibiotic resistance threat.

1.3 AIMS

The emergence of PDR *A. baumannii* severely diminishes the treatment options for this opportunistic pathogen. With a growing interest in the use of phages, several phages that infect *A. baumannii* have been identified and characterized. However, their restricted spectrum (killing only ~60% of *A. baumannii* isolates) limits the effectiveness of such phages as therapeutic agents (55-57). By comparison, the lysins are active against *A. baumannii* as a species and those with higher bactericidal activities comprise an N-terminal catalytic domain and a highly positively charged C-terminal peptide (46, 47). Considering the atypical domain composition, we tested the hypothesis that the peptide contributes to the lysins' activities by destabilizing the outer and inner membranes. We also aim to investigate the applicability of such peptides as AMPs against drug resistant *A. baumannii*.

To achieve these objectives, we characterized the positively charged C-terminus of *A. baumannii* phage lysin PlyF307 as P307. We also designed four derivatives and performed bactericidal assays to compare their activities. For the most active derivative and P307, we determined their minimum inhibitory concentrations (MIC) and synergies with antibiotics. After examining their selectivity in permeabilizing membranes, toxicity and serum tolerance, we proceeded to study their effectiveness in clearing *A. baumannii* from mouse skin infections. With this study, we aim to demonstrate the prospect of using peptide derivatives from lysins as antibacterial agents against Gram-negative pathogens.

2 CHAPTER 2 – LYSIN-BASED ANTIMICROBIAL PEPTIDES

2.1 MATERIALS AND METHODS

2.1.1 Peptides

2.1.1.1 Identification, modifications and structural predictions

Previously published works on phage lysins against Gram-negative bacteria (46, 47) suggested that the C-terminal portions of the lysins might destabilize the bacterial outer membrane to facilitate access to the peptidoglycan which is the lysin's substrate (Figure 2.1). Specifically, the highly cationic C-terminal region of *A. baumannii* phage lysin LysAB2 was speculated to be involved in permeabilizing the outer membrane (46). A similar highly positively charged sequence was identified in one of *A. baumannii* phage lysins isolated in our laboratory. This peptide was named P307, and it extends from amino acids 108-138 in PlyF307 (47), and resembles the LysAB2 peptide in terms of length and charge, but sharing only 41.2% similarity and 17.6% identity (MacVector ClustalW alignment).

P307 was modified with the eight amino acids constituting the full C-terminal part of native PlyF307, forming peptide $P307_{AE\text{-}8}$. In addition, eight amino acids (SQSRESQC) were fused to the C-terminus of P307 to yield $P307_{SQ\text{-}8C}$. This modification was based on the observation of an earlier study showing that the lack of these eight amino acids reduces the activity spectrum of the antimicrobial peptide HBc ARD (52) against Gram-negative bacteria. Two additional modifications of $P307_{SQ\text{-}8C}$ were also generated by: scrambling the sequence of the last eight amino acids to CSQRQSES ($P307_{CS\text{-}8}$); and changing the last amino acid from C to A ($P307_{SQ\text{-}8A}$). The sequence was scrambled to evaluate the importance of a specific sequence and the

cysteine change was introduced to examine the importance of intermolecular disulfide bond formation for activity. The amino acid sequences of the peptides are summarized in Table 2.1.

The structures of PlyF307 and $P307_{SQ\text{-}8C}$ were predicted by I-TASSER server (Zhang Lab, University of Michigan) (58-60) and the helical wheel plot for $P307_{SQ\text{-}8C}$ was created by NetWheels web application (61).

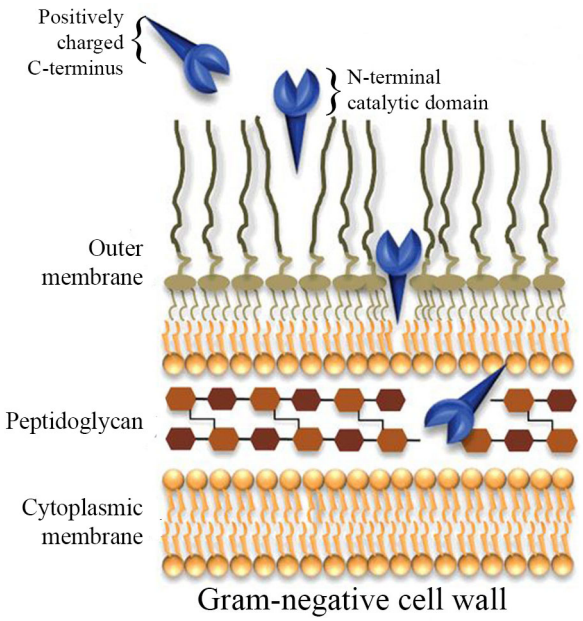

Figure 2.1 Permeabilization of outer membrane by Gram-negative lysin.

The cluster of positively charged amino acids at the C-terminus has been hypothesized to allow the lysin to traverse the outer membrane to reach the peptidoglycan. Upon contact with the peptidoglycan, the catalytic domain cleaves specific bonds resulting in hypotonic lysis and death. Adapted by permission from Portland Press: Biochemical Society Transactions (62), copyright 2016.

Table 2.1 Peptide derivatives of PlyF307

Names	Amino acid sequences
PlyF307	146 amino acids (GenBank Accession Number KJ740396)
P307	NAKDYKGAAAEFPKWNKAGGRVLAGLVKRRK *(108^{th}-138^{th})*
$P307_{AE-8}$	NAKDYKGAAAEFPKWNKAGGRVLAGLVKRRK**AEMELFLK** *(original)*
$P307_{SQ-8C}$	NAKDYKGAAAEFPKWNKAGGRVLAGLVKRRK**SQSRESQC** *(from Hep B)*
$P307_{CS-8}$	NAKDYKGAAAEFPKWNKAGGRVLAGLVKRRK**CSQRQSES** *(scramble)*
$P307_{SQ-8A}$	NAKDYKGAAAEFPKWNKAGGRVLAGLVKRRK**SQSRESQA** *(C39A)*

2.1.1.2 Synthesis

Peptides were synthesized at The Rockefeller University Proteomics Resource Center. All peptides were created using a Protein Technologies Symphony™ peptide synthesizer (PTI Tucson, Arizona, USA) on pre-coupled Wang (*p*-alkoxy-benzyl alcohol) resin (Bachem, Torrance, CA, USA). Reaction vessels were loaded at 25 μM and peptides were elongated using Fmoc protected amino acids (Anaspec, San Jose, CA, USA) (63). Deprotection of the amine was accomplished with 20% piperidine (Sigma-Aldrich) in NMP (N-methylpyrrolidinone). Repetitive coupling reactions were conducted using 0.6 M HATU/Cl-HOBT (azabenzotriazol tetramethyluronium hexafluorophosphate/6-chloro-1-hydroxybenzotriazole)(P3 Biosystems, Shelbyville, KY, USA) and 0.4 M NMM (N-methylmorpholine) using NMP (EMD) as the primary solvent (64). Resin cleavage and side-chain deprotection were achieved by transferring to a 100 mL round bottom flask and reacted with 4.0 mL concentrated, sequencing grade, trifluoracetic acid (Fisher) with triisopropylsilane (Fluka), degassed water, and 3,6-dioxa-1,8-octanedithiol (DODT, Sigma-Aldrich) in a ratio of 95:2:2:1 over a 6 h time frame. This was followed by column filtration to a 50 mL round bottom flask and TFA volume

reduced to 2 mL using a rotary evaporator. A standard ether precipitation was performed on the individual peptides by transferring to a 50 mL falcon tube containing 40 mL cold tert-butyl methyl ether (TBME, Sigma-Aldrich). Samples were placed in an ice bath for 2 h to aid precipitation followed by pellet formation using centrifugation (3300 rpm, 5 min). Excess ether was removed by vacuum aspiration and the peptide pellets were allowed to dry overnight in a fume hood. Dried peptide pellets were resolved in 20% acetonitrile and 10 mL HPLC grade water, subsampled for LC/MS and lyophilized. All crude products were subsequently analyzed by reverse-phase Aquity™ UPLC (Waters Chromatography, Milford, MA, USA) using a Waters BEH C18 column. Individual peptide integrity was verified by tandem electrospray mass spectrometry using a ThermoFinnigan LTQ™ (Thermo Fisher, Waltham, MA, USA) spectrometer system. Preparative chromatography was accomplished on a Vydac C18 RP preparative column on a Waters 600 Prep HPLC. Individual fractions were collected in 30 s intervals, characterized using LC/MS and fractions containing desired product were lyophilized. These were stored at -20°C until being re-suspended in autoclaved Milli-Q water for various assays. The stock solutions were then stored at 4°C.

2.1.2 Activity

2.1.2.1 Bacterial strains and growth conditions

A. baumannii strains in this study include clinical isolates from Hospital for Special Surgery in New York (#1775-#1799) (47), Ohio State University (S1, S3 and S5 provided by Dr. Vijay Pancholi), and ATCC® 17978™ from American Type Culture Collection. Bacteria were cultured in Trypticase Soy Broth or Brain Heart Infusion (TSB or BHI; Thermo Fisher Scientific, Waltham, MA, USA) at 37°C with aeration (200 rpm).

Stationary phase bacteria were cultured overnight while log phase bacteria were grown for 3 h in fresh media from 100x dilutions of overnight cultures. Strains for determining the specificity of the antimicrobial peptides were cultured under the same conditions, at the temperatures indicated: *B. anthracis* ΔSterne (30°C), *E. coli* DH5α (37°C), *K. pneumoniae* ATCC® 700603™ and 10031™ (37°C), *P. aeruginosa* PAO1 (30°C), and *S. aureus* RN4220 (30°C).

Biofilms were set up as previously described (47). Briefly, an overnight culture of *A. baumannii* strain #1791 was diluted 1000x (~10^5 cfu/mL) in TSB containing 0.2% glucose and incubated at 37°C for 72 h in ~2.5 cm segments of PVC catheter tubing (CareFusion) with the ends clamped shut to prevent evaporation. The catheter biofilms were washed with autoclaved Milli-Q water to remove planktonic cells before peptide treatment. Crystal violet (0.1%) was used to detect the presence of biofilm.

2.1.2.2 Bactericidal assays

Unless otherwise indicated, stationary phase bacteria (overnight cultures) were used for the assays. Bacteria were washed in assay buffer, re-suspended to ~10^6 cfu/mL, mixed with each antimicrobial peptide and incubated for 2 h at room temperature (22-25°C). After treatment, the reactions were serially diluted and plated for enumeration. Influencing factors on the activities of the peptides (P307 and $P307_{SQ-8C}$) were examined: buffer (50 mM sodium phosphate or Tris-HCl, pH 6.8-8.8; NaCl (0-200 mM); concentration (0-125 μg/mL P307); time (1-120 min); specificity (the bacterial strains mentioned above); and growth phase (log, stationary and biofilm). The buffer system for the experiments with the latter five factors was 50 mM Tris-HCl, pH 7.5. The biofilm-associated bacteria were re-suspended by thoroughly scraping the catheter tubing and

vortexing for 1 min. Experiments were conducted at least in triplicate and representative data are shown as mean + standard deviation. The black horizontal lines mark the limit of detection.

2.1.2.3 MIC, resistance and synergy assays

The broth microdilution method was used (65) to determine the MICs of levofloxacin, ceftazidime, polymyxin B, P307 and $P307_{SQ-8C}$ for *A. baumannii* strains #1791, #1798, S5 and ATCC17978. For the antibiotics, 1.5–2 fold serial dilutions (three lower and three higher) of the MICs determined by Etest (47) were included. For the peptides, two-fold serial dilutions (2000–31.25 μg/mL) were tested. Overnight cultures were re-suspended to ~10^5 cfu/mL in Mueller Hinton broth (pH 7.9). Antibiotics or peptides were added to a final volume of 100 μL for each dilution. Bacteria were allowed to grow at 37°C for 24 h at 220 rpm. The absorbance at 595 nm was then read in a SpectraMax Plus Reader (Molecular Devices). The MICs were determined as the lowest concentrations of antimicrobial agents that visibly inhibited bacterial growth. In addition, Alamar®Blue was used to confirm the data obtained from OD_{595}. Each experiment was repeated at least twice in duplicate.

Resistance development was investigated for P307, $P307_{SQ-8C}$ and polymyxin B with modifications to a published protocol (37). Briefly, *A. baumannii* strain #1791 was grown in two-fold serial dilutions (0.25× to 2× MIC) of the antimicrobial agents. The cultures commenced with 10^5 cfu/mL in MH broth (pH 7.9) as described above. The next day, each thriving culture in the highest concentration well was taken through the process again with two-fold serial dilutions (0.25× to 2× MIC) of respective antimicrobial agents and 10^5 cfu/mL starting culture. The process was repeated 7 times.

To investigate whether synergy exists between each peptide and antibiotic, checkerboard assays were conducted by mixing fractional inhibitory concentrations (FICs) of antibiotics (levofloxacin, ceftazidime and polymyxin B) with those of peptides P307 and $P307_{SQ-8C}$ as previously described (66). Isobolograms were constructed to determine the fractional inhibitory concentration indices (FICIs). Each experiment was repeated at least three times.

2.2 RESULTS

2.2.1 Structural analyses of peptides

The predicted structures of PlyF307 and P307$_{SQ\text{-}8C}$ suggested that the peptides form a “hairpin-like” di-alpha helical structure connected with a flexible linker region and the helical wheel plot suggested an amphipathic helix motif (Figure 2.2).

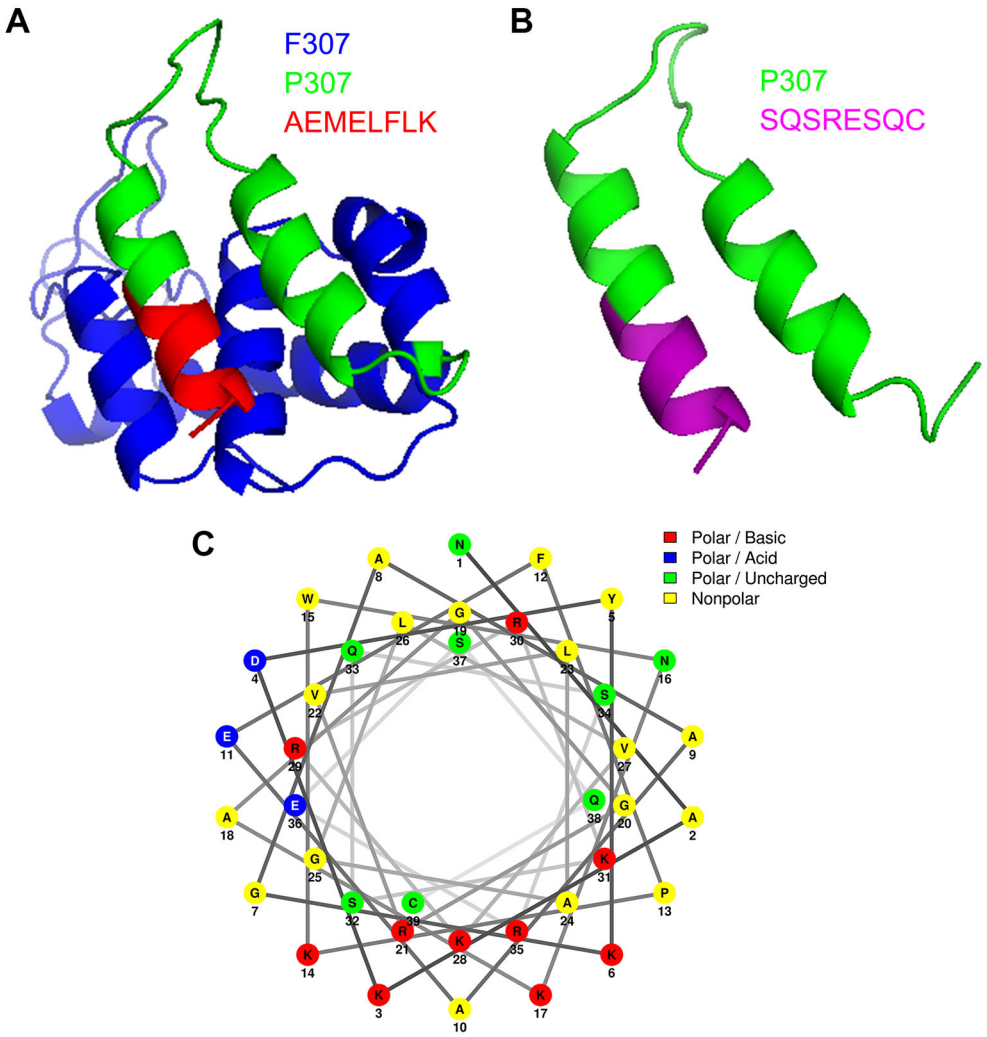

Figure 2.2 Structural analyses.

Predictions of (A) PlyF307 and (B) P307$_{SQ\text{-}8C}$ by I-TASSER server (58-60). (C) Helix wheel plot of P307$_{SQ\text{-}8C}$ by NetWheels web application (61).

2.2.2 Activity

2.2.2.1 Bactericidal assays

First the bactericidal activities of the peptides P307, $P307_{AE-8}$ and $P307_{SQ-8C}$ were compared. $P307_{SQ-8C}$ was the most active, reducing ~10^6 cfu/mL of bacteria to below the limit of detection (<10 cfu/mL). P307 was slightly more active than $P307_{AE-8}$, but both peptides induced ~3.8-log decreases in viability (Figure 2.3A). Since $P307_{SQ-8C}$ was the most active, the importance of the last eight amino acids SQSRESQC was investigated. To test whether the linkage between P307 and the eight-amino-acid peptide was important, the activities were compared among P307, $P307_{SQ-8C}$, the combination of P307 and equimolar concentrations of the SQSRESQC peptide and the SQSRESQC peptide alone. The combination was only as active as P307 while the SQSRESQC peptide alone had no activity (Figure 2.3B). Hence the linkage was essential for the high bactericidal activity of $P307_{SQ-8C}$. Next, the importance of sequence and composition was investigated by synthesizing $P307_{CS-8}$ with the last eight amino acids in $P307_{SQ-8C}$ scrambled to CSQRQSES. The bactericidal activities of $P307_{SQ-8C}$ and $P307_{CS-8}$ were comparable (Figure 2.3C), indicating that the amino acid composition was more important than the sequence for the superior activity of $P307_{SQ-8C}$. For further investigation, we used $P307_{SQ-8C}$ since it was the most active, and compared its activity to P307.

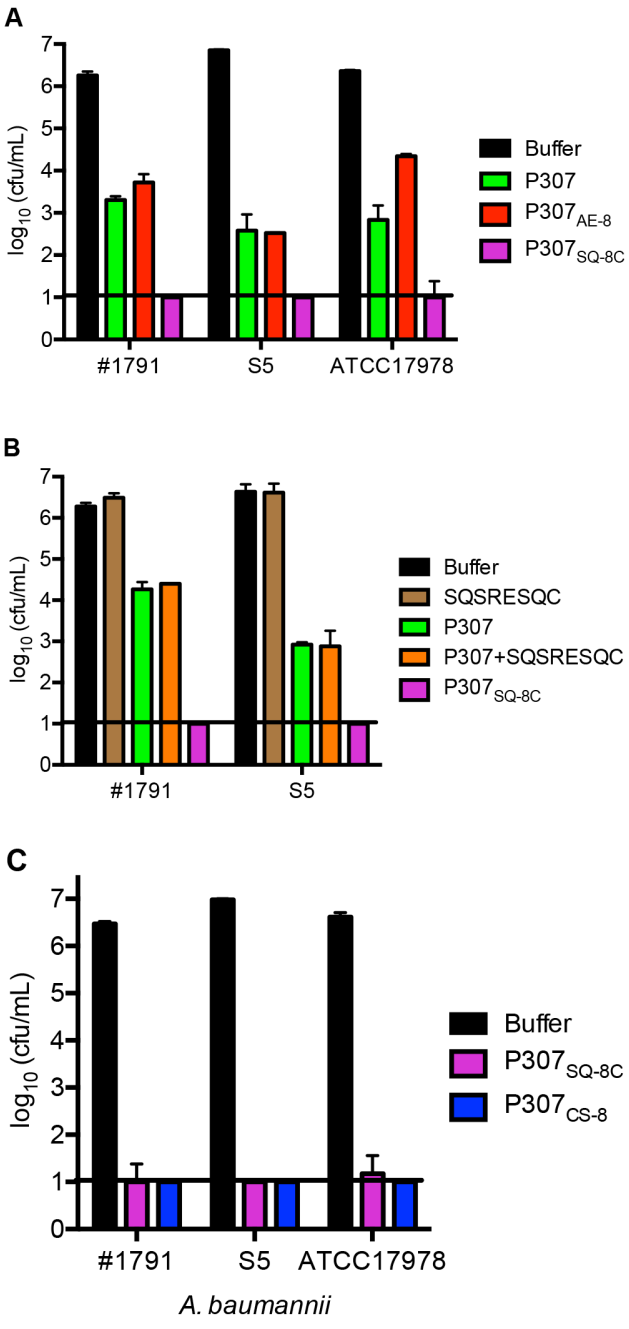

Figure 2.3 Comparison of *in vitro* bactericidal activities of peptides. Bacteria were treated with 50 µg/mL of each peptide for 2 h at 22-25°C. Serial dilutions were plated for cfu counting. (A) The bactericidal activities of P307 and its variants $P307_{AE-8}$ and $P307_{SQ-8C}$ against *A. baumannii* strains #1791, S5 and ATCC17978. (B) The activities of P307, $P307_{SQ-8C}$, and equimolar SQSRESQC peptide with and without P307 against strains #1791 and S5. (C) The activities of $P307_{SQ-8C}$ and a scramble variant $P307_{CS-8}$ against strains #1791, S5 and ATCC17978. The error bars show standard deviation and the black horizontal line marks the limit of detection.

The effects of pH and NaCl on the *in vitro* activities of P307 and $P307_{SQ-8C}$ were investigated. *A. baumannii* strain #1791 was treated with 50 μg/mL of either peptide in the presence of varying pH and salt conditions. Using two buffer systems (sodium phosphate and Tris-HCl), pH 6.8, 7.5, 8.0 and 8.8 were compared. The peptides were more active in Tris-HCl buffer and higher pH values elicited better killing (Figure 2.4A). Thus, the *in vitro* experiments were continued with 50 mM Tris-HCl, pH 7.5 to approximate physiological pH. The activities of both peptides were inversely proportional to the concentration of NaCl (Figure 2.4B). When titration and killing kinetics were investigated, the activities of both peptides were concentration-dependent (Figure 2.4C) and $P307_{SQ-8C}$ acted faster than P307, resulting in ~3.2-log decrease after 5 min, with a continued reduction in bacterial count up to ~5 logs 120 min after $P307_{SQ-8C}$ addition (Figure 2.4D). There was no difference in activities of both peptides either at room temperature (22-25°C) or 37°C and they retained activity after being heated at 95ºC for 1 h (data not shown). From these *in vitro* characterization experiments, the optimal experimental conditions were chosen to be 50 μg/mL peptides in 50 mM Tris-HCl, pH 7.5 for 2 h at 22-25°C, unless otherwise indicated.

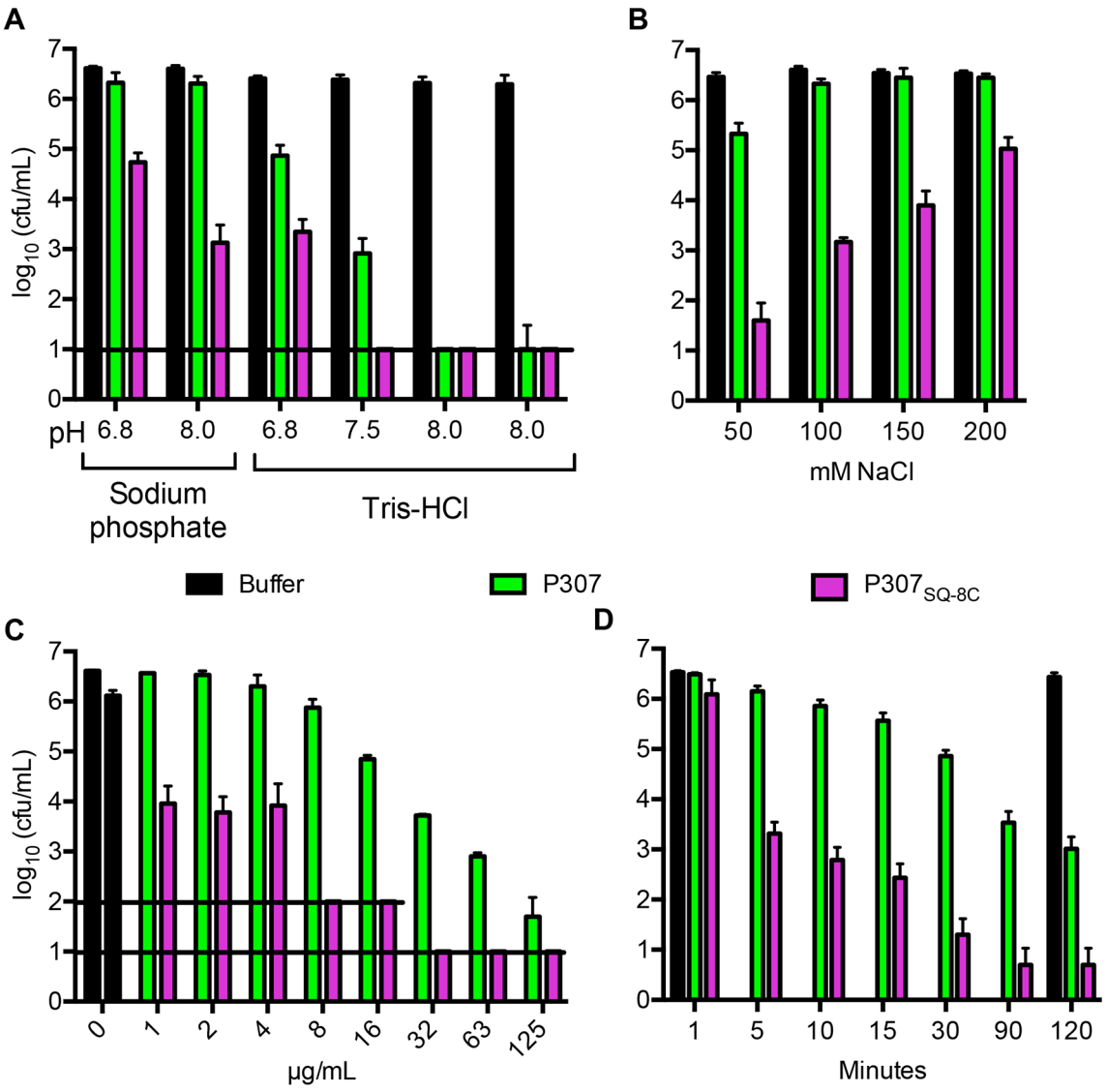

Figure 2.4 *In vitro* bactericidal activities of P307 and P307$_{SQ-8C}$.

A. baumannii strain #1791 was treated with 50 µg/mL of P307 or P307$_{SQ-8C}$ for 2 h at 22-25°C to investigate the optimal (A) pH and (B) NaCl concentration for killing. The same conditions, except for the variables, were used with 50 mM Tris-HCl, pH 7.5 to determine the (C) optimal killing concentration, and (D) killing kinetics. The error bars show standard deviation and the black horizontal line marks the limit of detection.

The *in vitro* bactericidal spectra of P307 and $P307_{SQ-8C}$ were also examined. Among the bacteria tested, *A. baumannii* strains were consistently the most sensitive to the peptides, showing an average of 2.7- and 6.2-log decrease with P307 and $P307_{SQ-8C}$, respectively. *Bacillus anthracis*, *Pseudomonas aeruginosa* and *Staphylococcus aureus* were moderately sensitive to P307 and $P307_{SQ-8C}$, with an average of ~1.3- and 2.9-log decrease, respectively. Both *E. coli* and *Klebsiella pneumoniae* were resistant to the peptides under these experimental conditions (Figure 2.5).

To examine the activity of each peptide against *A. baumannii* at different growth phases, the sensitivities of strain #1791 were compared at log phase, stationary phase and in biofilms. The log phase organisms were slightly more sensitive to P307 than stationary phase (~3.7- versus 2.4-log decrease) (Figure 2.6A). However, no such difference was observed for $P307_{SQ-8C}$, with both growth phases being equally sensitive to the maximal killing effect of the $P307_{SQ-8C}$ (>5-log decrease). Biofilm-associated *A. baumannii* was more resistant (Figure 2.6B). Biofilms were treated with 250 μg/mL P307 or $P307_{SQ-8C}$ for 2 or 24 h. After 2 h, ~3- and 4-log decrease in cfu/mL was observed with P307 and $P307_{SQ-8C}$, respectively. After 24 h, an additional ~1.3-log decrease was observed with P307 while there was no further decrease with $P307_{SQ-8C}$.

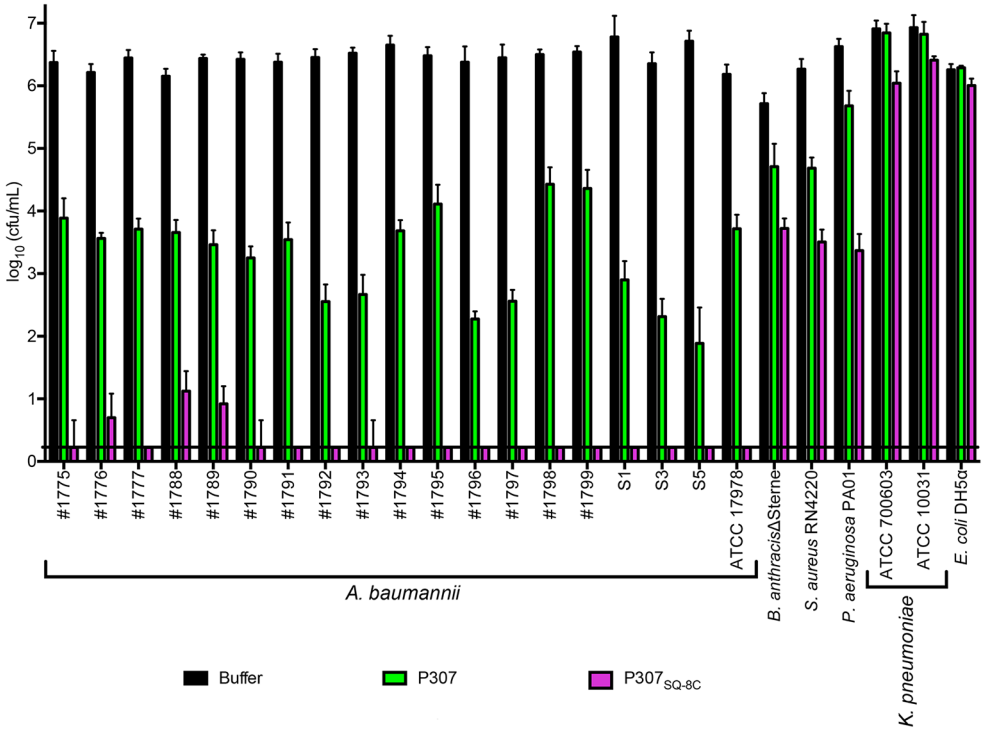

Figure 2.5 *In vitro* bactericidal spectra of P307 and P307$_{SQ-8C}$.

Different bacterial species (*A. baumannii*, *B. anthracis*, *E. coli*, *P. aeruginosa*, *S. aureus* and *K. pneumoniae*) were treated with 50 μg/mL of P307 or P307$_{SQ-8C}$ in 50 mM Tris-HCl, pH 7.5 for 2 h at 22-25°C to investigate the specificity of the peptides. Serial dilutions were plated for cfu counting. The error bars show standard deviation and the black horizontal line marks the limit of detection.

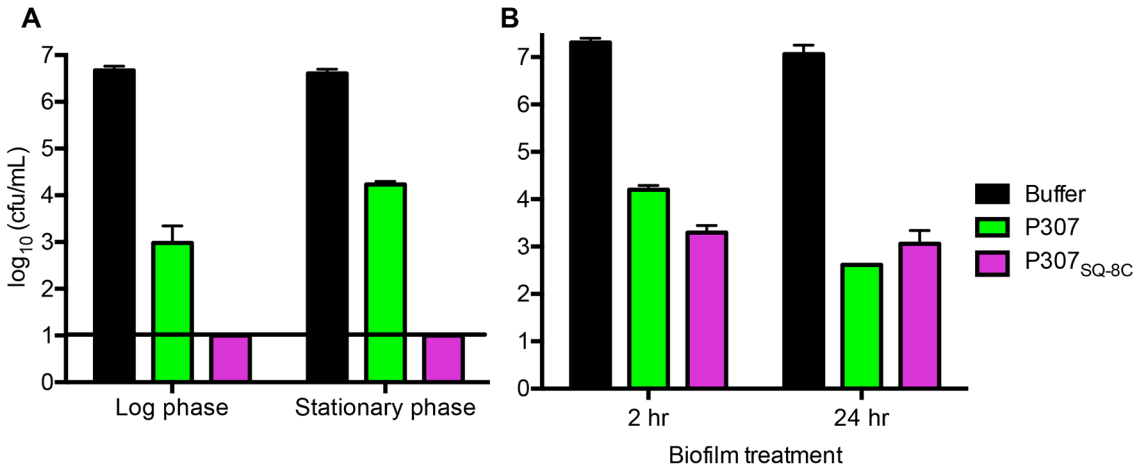

Figure 2.6 Bactericidal activities of P307 and $P307_{SQ-8C}$ against *A. baumannii* strain #1791 in log phase, late-stationary phase and biofilm.

(A) Bacteria in log phase and late stationary phase were treated with 50 μg/mL of P307 or $P307_{SQ-8C}$ for 2 h at 22-25°C. (B) *A. baumannii* biofilms in PVC catheters were treated with 250 μg/mL of P307 or $P307_{SQ-8C}$ for 2 or 24 h at 22-25°C. Serial dilutions were plated for cfu counting. The error bars show standard deviation and the black horizontal line marks the limit of detection.

2.2.2.2 MIC, resistance and synergy assays

In order to compare the efficiency of the peptides with clinically used antibiotics, minimal inhibitory concentration (MIC) assays were performed on four *A. baumannii* strains: #1791, #1798, S5 and ATCC17978. The strains displayed varying degrees of sensitivity to levofloxacin, ceftazidime and P307 while the MICs of polymyxin B and $P307_{SQ-8C}$ were more consistent (Table 2.2). $P307_{SQ-8C}$ had a lower MIC than P307, which was in accordance with *in vitro* killing activity (Figure 2.3 and 2.5).

No resistance was observed for any of the antimicrobial agents. However since the starting culture was 10^5 cfu/mL, it is likely that the frequency of resistant clone development was not high enough to be detected.

The synergistic effects were examined between each peptide and levofloxacin, ceftazidime or polymyxin B by the checkerboard method (isobologram). No synergy was observed between either peptide and levofloxacin or ceftazidime (data not shown). However, polymyxin B acted synergistically with both P307 and $P307_{SQ-8C}$ (FICIs = 0.125, <0.5).

Table 2.2 MIC comparison of peptides and antibiotics examined in this study

A. baumannii strains	Levofloxacin		Ceftazidime		Polymyxin B		P307		$P307_{SQ-8C}$	
	µg/mL	µM	µg/mL	µM	µg/mL	µM	µg/mL	µM	µg/mL	µM
#1791	6	16.6	**128**	**234**	0.25	0.19	750	221	62.5	14.5
#1798	**32**	**88.6**	**>1024**	**>1873**	0.25	0.19	1000	294	62.5	14.5
S5	6	16.6	**64**	**117**	0.25	0.19	2000	588	125	29
ATCC17978	0.075	0.21	6	11	0.25	0.19	750	221	125	29

2.3 ACKNOWLEDGMENTS

I would like to thank Dr. Rolf Lood and Benjamin Y. Winer for their invaluable contributions in designing peptides. I am also grateful to Dr. Vijay Pancholi for *A. baumannii* strains and Dr. Henry A Zebroski III (Rockefeller University Proteomics Resource Center) for the peptides. I thank Ravenne Reid for her excellent assistance.

3 CHAPTER 3 – INFLUENCING FACTORS ON BACTERICIDAL ACTIVITIES

3.1 MATERIALS AND METHODS

3.1.1 Inter-peptide disulfide bond formation

The contribution of disulfide bond formation to the increased activity of $P307_{SQ-8C}$ was investigated by comparing with $P307_{SQ-8A}$ in the presence of the reducing agent TCEP (0.1 and 1 mM) (Tris (2-carboxyethyl) phosphine hydrochloride solution)(Sigma). Experiments were conducted at least in triplicate and representative data are shown as mean + standard deviation.

3.1.2 pH-dependent sensitivity of *E. coli* and *K. pneumoniae*

The least sensitive Gram-negative species at pH 7.5 (Figure 2.5) were treated with 50μg/mL P307 or $P307_{SQ-8C}$ at pH 8.8. Experiments were conducted at least in triplicate and representative data are shown as mean + standard deviation. The black horizontal line marks the limit of detection.

3.1.3 DNA-binding assay

The affinity of peptide P307 for DNA was investigated by electrophoretic mobility shift assay (67). P307 was mixed with 50 ng of random DNA (1 kb amplicon of *Bdellovibrio* genomic DNA) at different peptide to DNA ratios (0:1-15:1) in a binding buffer (5 mM Tris-HCl, pH 8.0, 10 mM EDTA, 5% glycerol, 20 mM KCl, 50 μg/mL BSA). As a positive control, a peptide from *Bdellovibrio bacteriovorus* that was previously found in our laboratory to have DNA-binding capacity (amino acid sequence – MASKTKKTEYIRERKKATSGKKRKAANRTKGTTKSAKTLFKD) was used

(unpublished results). After incubation for 1 h at 22-25°C, the peptide and DNA mixture was analyzed by Agarose gel electrophoresis (67).

3.1.4 Transmission electron microscopy (TEM)

An overnight culture of A. baumannii strain #1791 was collected, washed in 50 mM Tris-HCl, pH 7.5 and re-suspended in the same buffer to ~10^8 cfu/mL. The bacteria were treated with buffer (control) or 300 μg/mL $P307_{SQ-8C}$ or 1 mg/mL lysozyme (from chicken egg white, lyophilized powder, protein ≥90%) (Sigma) or 300 μg/mL $P307_{SQ-8C}$ and 1 mg/mL lysozyme combined for 5 min or 2 h. The samples were fixed with 2.5% glyceraldehyde in 0.1 M sodium cacodylate, and then TEM images were taken at magnification ×3300 or ×6600. Representative figures are shown.

3.1.5 SYTOX green uptake assay

The permeability of bacterial membrane upon peptide treatment was measured by SYTOX® Green uptake (52). Briefly, overnight cultures of bacteria were washed and re-suspended to ~10^7 cfu/mL in 50 mM Tris-HCl pH 7.5. Benzonase® nuclease (25 U/mL)(Novagen) and SYTOX® Green (1 μM)(Invitrogen) was added to the bacterial cells, and incubated for 15 min at 22-25°C in the dark. Peptides (50 μg/mL; 14.7 μM P307 and 11.6 μM $P307_{SQ-8C}$) were added. Polymyxin B (2 μg/mL)(Sigma) was used as a control (68). Relative fluorescence units (RFU) were measured in a SpectraMax Plus reader (Molecular Devices) at 22-25°C (ex: 485 nm, em: 520 nm) for 2 h. Experiments were carried out twice in duplicate and representative data are shown as mean ± standard deviation.

3.2 RESULTS

3.2.1 Inter-peptide disulfide bond formation

Since $P307_{SQ-8C}$ contained a C-terminal cysteine, the importance of disulfide bond formation for the high activity of $P307_{SQ-8C}$ was investigated. SDS-PAGE analysis showed that a portion of $P307_{SQ-8C}$ (~5-10%) ran at twice the theoretical molecular weight (MW) of this peptide while all of $P307_{SQ-8A}$ ran at the theoretical MW (data not shown), suggesting a role for disulfide bond formation. To examine this, the C-terminal cysteine residue of $P307_{SQ-8C}$ (the only cysteine in this peptide) was changed to alanine. The resulting alanine variant, $P307_{SQ-8A}$, ran at the expected size for a peptide monomer (4.3 kDa) with no observable band at the dimer location by SDS-PAGE (data not shown). The difference in bactericidal activities of $P307_{SQ-8A}$ and $P307_{SQ-8C}$ were compared within the limit of detection by using 10 μg/mL peptides instead of 50 μg/mL. Furthermore, TCEP (0.1 and 1 mM) was added to specifically reduce disulfide bonds. Without TCEP, $P307_{SQ-8C}$ was more active than $P307_{SQ-8A}$ (~5- versus ~2.7-log decrease) (Figure 3.1). The addition of TCEP did not affect $P307_{SQ-8A}$ while the activity of $P307_{SQ-8C}$ was reduced by ~2 logs. However, $P307_{SQ-8A}$ was still more active than P307, suggesting that although disulfide bond formation was important, it was not the only contributing factor for the superior activity of $P307_{SQ-8C}$.

3.2.2 pH-dependent sensitivity of *E. coli* and *K. pneumoniae*

Among the Gram-negative species examined, *E. coli* and *K. pneumoniae* were the least sensitive to the peptides at pH 7.5 (Figure 2.5). However, at pH 8.8, both were sensitive to 50 μg/mL of the peptides (Figure 3.2), indicating the electrostatic interactions between the peptides and bacterial membrane.

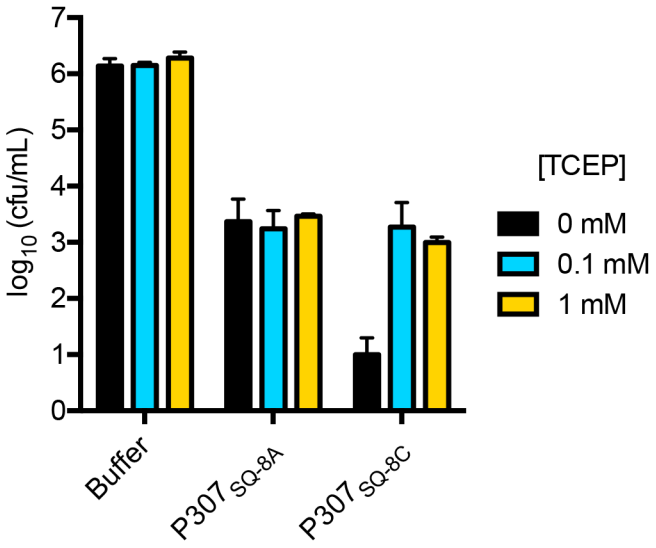

Figure 3.1 The importance of terminal cysteine and its disulfide bond formation for bactericidal activity of $P307_{SQ\text{-}8C}$.

A. baumannii strain #1791 was treated with 10 μg/mL $P307_{SQ\text{-}8A}$ (with Ala instead of Cys at the C-terminus) or $P307_{SQ\text{-}8C}$ in 50 mM Tris-HCl, pH 7.5 with or without TCEP for 2 h at 22-25°C. Serial dilutions were plated for cfu counting. The error bars show standard deviation.

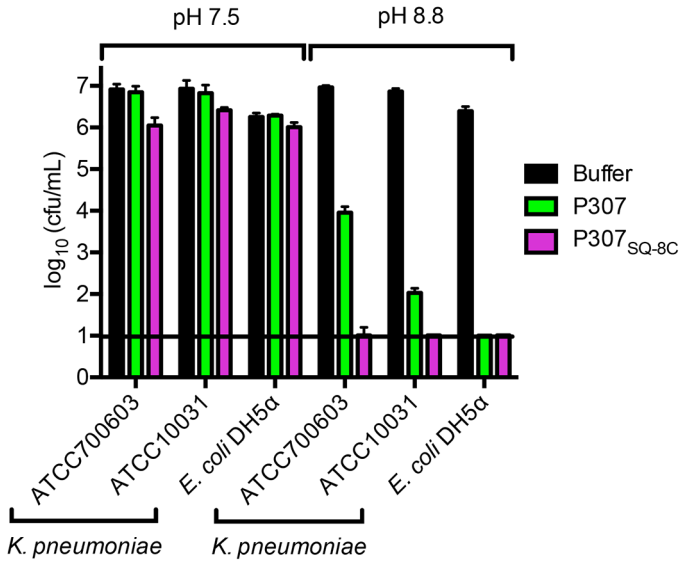

Figure 3.2 Bactericidal activities of P307 and $P307_{SQ-8C}$ against *K. pneumoniae* and *E. coli* at pH 7.5 and 8.8.

The bacteria were treated with 50 μg/mL peptides in 50 mM Tris-HCl for 2 h at 22-25°C. Serial dilutions were plated for cfu counting. The error bars show standard deviation and the black horizontal line marks the limit of detection.

3.2.3 DNA-binding assay

Due to the presence of several cationic residues on the peptides (net charge of +7), their effects on DNA were investigated. The affinity of P307 for DNA was examined by electrophoretic mobility shift assay. There was no shift in molecular weight at all ratios of P307 to DNA tested whereas a positive control peptide known to bind DNA caused a clear shift in electrophoretic mobility (Figure 3.3).

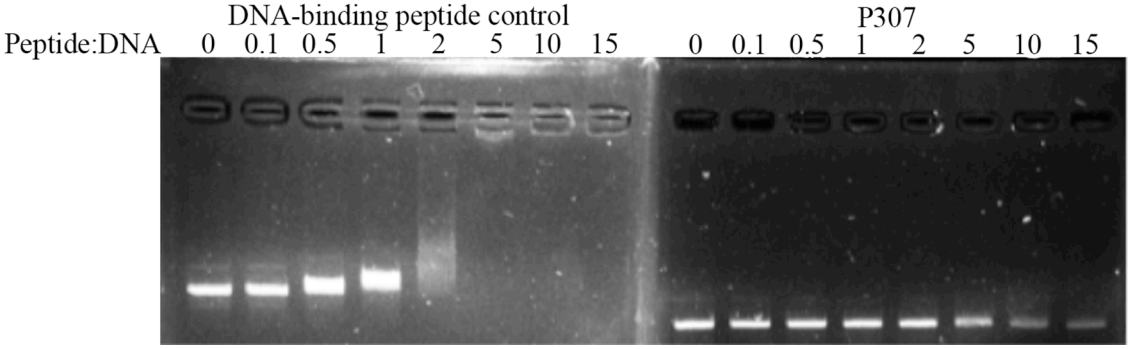

Figure 3.3 Affinity of P307 for DNA.

The peptide P307 was mixed with DNA at different peptide:DNA ratios (0:1-15:1) and incubated for 1 h before being analyzed on an Agarose gel. In comparison to positive control peptide, no electrophoretic shift was observed for P307.

3.2.4 Transmission electron microscopy (TEM)

Another negatively charged bacterial component investigated was bacterial membrane. TEM was used to visualize the effects of $P307_{SQ-8C}$ on *A. baumannii* membrane. The samples were prepared by treating *A. baumannii* strain #1791 with buffer (control) or 300 μg/mL $P307_{SQ-8C}$ or 1 mg/mL lysozyme or peptide and lysozyme combined for 5 min or 2 h. A comparison of the TEM images revealed that treatment with $P307_{SQ-8C}$ led to: 1) membrane blebbing and changes in intracellular density, 2) appearance of 'intact bacterial ghosts', and 3) occasional disruption of the cell wall and cytoplasmic membrane (Figure 3.4A, B and C). On the other hand, lysozyme hydrolyzed the peptidoglycan and released the cellular content (Figure 3.4D). Finally, the combined treatment resulted in complete debris formation as $P307_{SQ-8C}$ and lysozyme destabilized the membrane and peptidoglycan simultaneously (Figure 3.4 E and F).

3.2.5 SYTOX green uptake assay

As our data suggested a killing mechanism by cytoplasmic membrane destabilization, the extent of bacterial membrane disruption by P307 and $P307_{SQ-8C}$ was measured using the SYTOX® Green uptake assay. Both peptides permeabilized the membranes of *A. baumannii* strain #1791 at pH 7.5 and *K. pneumoniae* strain ATCC700603 at pH 8.8, giving rise to an increase in fluorescent signals of SYTOX® Green dye as it bound to intracellular DNA. In contrast, the signal increase was minimal for *K. pneumoniae* ATCC700603 at pH 7.5 (Figure 3.5). The results were consistent with the difference in sensitivities of the bacterial species at different pH (Figures 2.5 and 3.2).

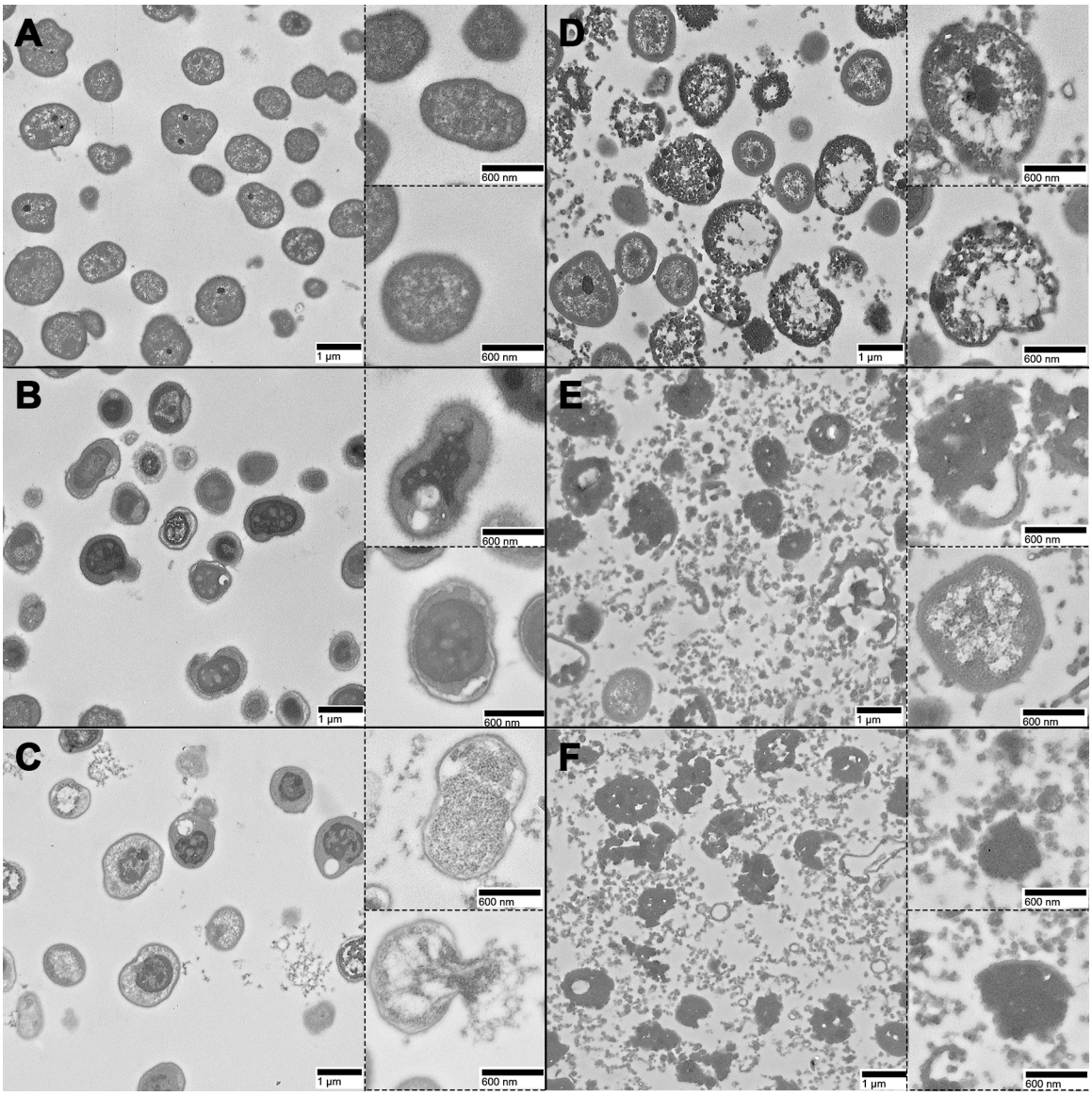

Figure 3.4 Representative TEM images.

A. baumanii strain #1791: untreated control (A), treated with 300 µg/mL $P307_{SQ-8C}$ for 5 min (B) and for 2 h (C), treated with 1 mg/mL lysozyme for 2 h (D), treated with 300 µg/mL $P307_{SQ-8C}$ and 1 mg/mL lysozyme for 5 min (E) and for 2 h (F). Magnification, × 3300 (left, scale bar = 1 µm) and ×6600 (right top and bottom, scale bar = 600 nm).

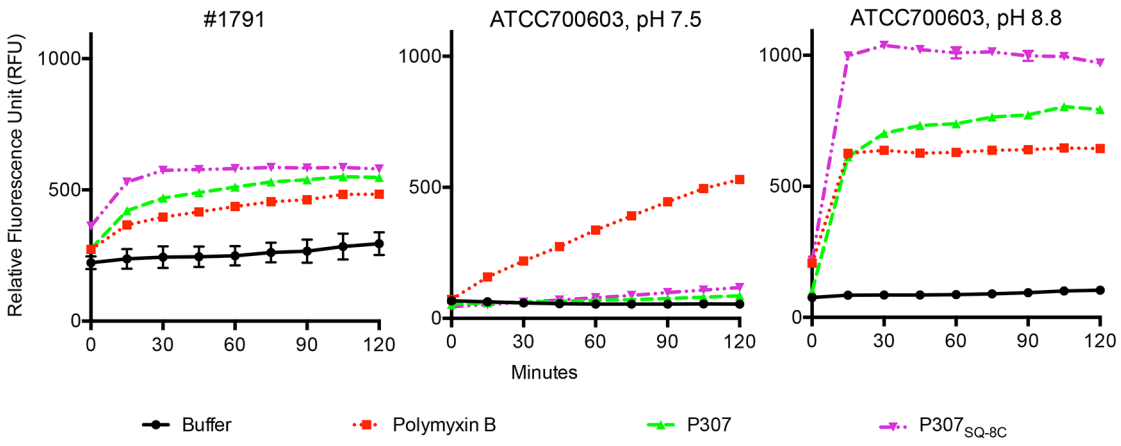

Figure 3.5 Membrane permeability of bacteria treated with P307 and P307$_{SQ-8C}$.

A. baumannii strains #1791 and *K. pneumoniae* strain ATCC700603 were treated in 50 mM Tris-HCl at indicated pH with 50 μg/mL of P307 or P307$_{SQ-8C}$ in the presence of 1 μM SYTOX® Green (Invitrogen). Benzonase® nuclease (25 U/mL)(Novagen) was also added to remove extracellular DNA. The permeability of bacterial membrane was monitored for 2 h by the increase in relative fluorescence units of SYTOX® Green dye, using polymyxin B as a positive control. The error bars show standard deviation.

3.3 ACKNOWLEDGMENTS

I would like to thank Dr. Ryan Hoselpoth for generously sharing TCEP and Douglas Deutch for conducting DNA-binding assay. I am especially grateful to Drs. Nadine Soplop and Kunihiro Uryu (Rockefeller University Electron Microscopy Resource Center) for the TEM images.

4 CHAPTER 4 – SAFETY AND *IN VIVO* ACTIVITY

4.1 MATERIALS AND METHODS

4.1.1 Cytotoxicity assays

The hemolytic assays were conducted as previously described (52). Briefly, human blood was gathered in an EDTA-tube, and red blood cells (RBC) were collected through low speed centrifugation. Cells were washed and re-suspended to a 10% RBC solution in PBS, and mixed with 80 μM (345 μg/mL) $P307_{SQ-8C}$. PBS and 1% Triton X-100 were used as negative and positive controls, respectively. After 1 h incubation at 37°C, the supernatant was collected, and the absorbance at 405 nm was recorded through SpectraMax Plus Reader (Molecular Devices) to measure the release of hemoglobin. The reactions were carried out twice in triplicate and representative data are shown as mean + standard deviation.

A human B lymphoblastoid cell line (LCL) obtained from The Rockefeller University was grown in RPMI media supplemented with L-glutamine and 10% fetal bovine serum. Cells were harvested by low speed centrifugation, washed and re-suspended in PBS to ~$5x10^6$ live cells/mL, as determined by trypan blue exclusion tests. LCL cells (~$5x10^5$) were incubated with 40, 80 and 120 μM $P307_{SQ-8C}$ at 37°C in a humidified 5% CO_2 atmosphere for one hour. The cells were then stained according to manufacturer's instructions (CellTiter 96 Non-radioactive cell proliferation assay, Promega) where live B cells reduced the dye to insoluble formazan for an additional 4 h. Solubilization/Stop solution was added and incubated at 37°C overnight. Next, the absorbance at 570 nm was measured in SpectraMax Plus Reader (Molecular Devices) to

quantitate B cell survival. Triton X-100 was used as a positive control. The reactions were carried out in triplicate and data are shown as mean + standard deviation.

4.1.2 Endotoxin assay

To detect the amount of endotoxin release, strain #1791 (~10^7 cfu/mL) was incubated at 22-25°C for 2 h with different concentrations of P307 or $P307_{SQ-8C}$. The samples were briefly centrifuged (2000 × g) for 1 min to remove live cells. All reagents were prepared in endotoxin-free autoclaved Milli-Q water. Endpoint Chromogenic LAL Assay (Lonza) was conducted according to manufacturer's instructions. Polymyxin B and 100% ethanol were used for comparison and positive control, respectively. The experiment was conducted twice in duplicate and representative data are shown as mean + standard deviation.

4.1.3 Bactericidal activity in plasma and its components

Human blood was collected in a heparin-tube and centrifuged. The supernatant was filtered and stored at 4°C overnight. The filtrate was centrifuged and filtered again to remove any debris. The resulting solution was used as 100% plasma. The components of plasma examined for interference were monovalent cation (Na^+), divalent cations (Ca^{2+} and Mg^{2+}) and albumin. Chloride salts of the cations and albumin from human serum (lyophilized powder, ≥ 97%)(Sigma) were prepared in Milli-Q water and sterile filtered. Bactericidal assays, as described above, were conducted in 100% plasma, and in buffered solutions (50 mM Tris-HCl, pH 7.5) containing 150 mM NaCl, 1 mM $CaCl_2$, 1 mM $MgCl_2$, and 50 mg/mL human serum albumin (HSA), using 100 µg/mL P307 or $P307_{SQ-8C}$. The experiments were conducted at least in triplicate and data are shown as mean + standard deviation.

4.1.4 Mouse skin infection

The Rockefeller University institutional animal care and use committee approved all *in vivo* protocols. Skin infection was induced with *A. baumannii* as previously described (69). Briefly, the backs of 30 female CD-1 mice (6 to 8 weeks of age; Charles River Laboratories) were shaved with an electric razor. Nair^{TM} depilatory cream was applied to the shaved areas to remove any remaining hair. The areas were then disinfected with alcohol wipes, and tape stripped with autoclave tape 20 times in succession, using a fresh piece of tape each time. The tape stripped areas were disinfected again with alcohol wipes. An area of ~ 1 cm^2 was then marked and infected with 10 μL of ~10^8 cfu/mL *A. baumannii* strain #1791. The bacteria were allowed to colonize for 16-18 h, after which the infected area was either left untreated or treated with 200 μg of $P307_{SQ\text{-}8C}$ or 2 μg of polymyxin B in autoclaved Milli-Q water for 2 h. To harvest the remaining bacteria on the skin, the mice were sacrificed and the infected skin was processed in 500 μL PBS for 1-2 min in a Stomacher® 80 Biomaster using a microbag (Seward Ltd., UK). The solution was serially diluted and plated on LB agar containing 4 μg/mL levofloxacin and 12 μg/mL ampicillin for selection. The resulting cfu/mL from each animal was plotted as an individual point and the horizontal bars represent the mean values. Data were analyzed using Ordinary one-way ANOVA in GraphPad Prism 6.0. The dotted horizontal line marks the limit of detection.

4.2 RESULTS

4.2.1 Cytotoxicity assays

Since membrane-acting antimicrobial peptides have been shown to be active against mammalian membranes (70), the cytotoxicity of the peptides were evaluated using human red blood cells (RBCs) and B cells. In contrast to the 1% Triton-X-100 positive control, 80 μM (345 μg/mL) $P307_{SQ-8C}$ did not lyse RBCs but killed *A. baumannii* strain #1791 (~4.8 logs) in PBS (Figure 4.1A). Similarly, the survival of B cells was not significantly affected by 40, 80 and 120 μM $P307_{SQ-8C}$ (Figure 4.1B).

4.2.2 Endotoxin assay

Even though the peptides did not display cytotoxicity against human RBCs, toxicity could possibly arise from the bacterial endotoxin released upon peptide treatment. Hence, the Endpoint Chromogenic LAL Assay (Lonza) was conducted to measure the amount of endotoxin released by *A. baumannii* strain #1791 after 2 h of incubation with peptides. The peptides generated endotoxin unit concentrations similar to that of the 100% ethanol positive control. Polymyxin B released more endotoxin at 0.5 μg/mL than at 2 μg/mL, but less than the peptides (Figure 4.2). This apparent reduced release was likely due to the known interaction of polymyxin B with lipid A (71), the active component for LAL assay. The peptides did not interfere with endotoxin detection (data not shown).

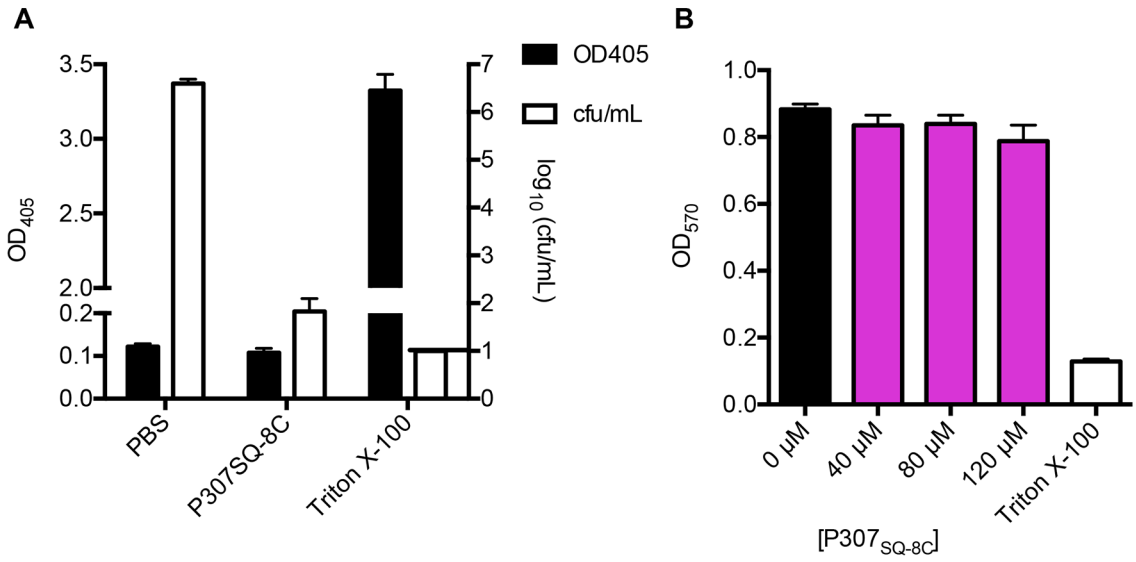

Figure 4.1 Cytotoxicity assays.

(A) Hemolysis. Red blood cells (RBCs) were incubated with 345 μg/mL $P307_{SQ-8C}$ in PBS and the release of hemoglobin into the supernatant was measured by OD_{405} to determine hemolysis, using 1% Triton X-100 as a positive control. The activity of $P307_{SQ-8C}$ was examined against *A. baumannii* strain #1791 under the same experimental conditions. (B) B cell survival. Live B cells (~$5x10^5$) were incubated with 172.5, 345 and 517.5 μg/mL $P307_{SQ-8C}$ for 1 h at 37°C in a humidified 5% CO_2 atmosphere. CellTiter 96® Non-Radioactive Cell Proliferation Assay (Promega) was conducted to quantify the survival of B cells, using 1% Triton X-100 as a positive control. The error bars show standard deviation and the black horizontal line marks the limit of detection for cfu/mL.

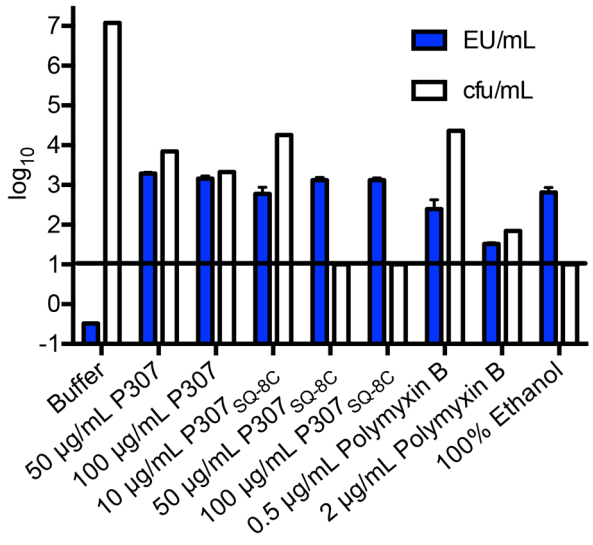

Figure 4.2 Endotoxin release.

A. baumannii strain #1791 (~10^7 cfu/mL) was treated with different concentrations of antibacterials for 2 h at 22-25°C. The samples were centrifuged to remove live cells. The supernatant was analyzed with the Endpoint Chromogenic LAL Assay (Lonza) to measure endotoxin units, using 100% ethanol as a positive control. The error bars show standard deviation and the black horizontal line marks the limit of detection for cfu/mL.

4.2.3 Bactericidal activity in plasma and its components

The activities of the peptides were examined in human blood plasma. Both P307 and $P307_{SQ\text{-}8C}$ (100 μg/mL) were inactive in 100% plasma. The activities in Tris buffer were also interfered to varying degrees by the addition of monovalent and divalent cations as well as human serum albumin at physiological concentrations (Figure 4.3).

4.2.4 Mouse skin infection

Since blood plasma interfered with the activities of both peptides, and the skin is a common route of infection by *A. baumannii*, the *in vivo* activity of $P307_{SQ\text{-}8C}$ was investigated using a mouse skin infection model. Skin abrasions were induced on the shaved backs of the mice by tape-stripping, and the irritated skin was infected with 10^6 cfu of *A. baumannii* strain #1791 for 16 h. The infected area was then treated with 2 μg polymyxin B or 200 μg $P307_{SQ\text{-}8C}$ for 2 h after which the infected skin was excised and processed for bacterial counts. Both treatments were found to significantly reduce the bacterial load (~2 logs) in the infected skin using this single dose ($P < 0.02$, Ordinary one-way ANOVA) (Figure 4.4).

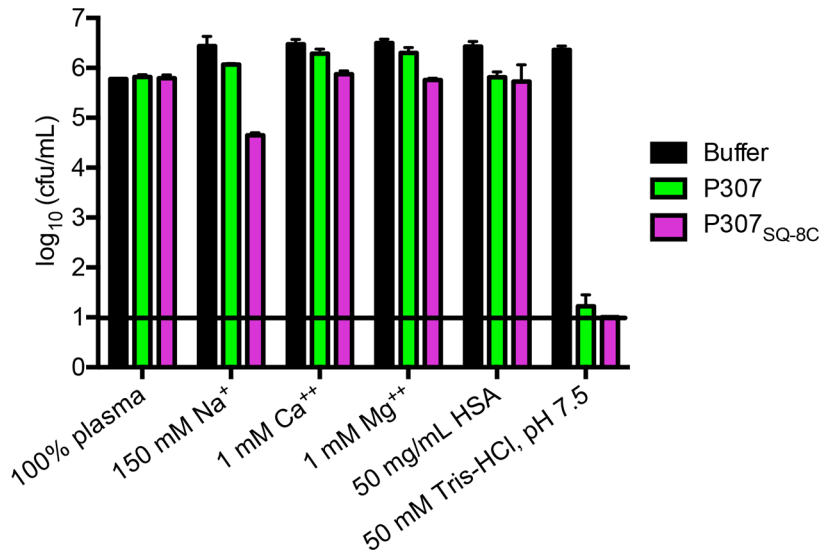

Figure 4.3 Activities of peptides in plasma and its components.

A. baumannii strain #1791 was treated with 50 µg/mL P307 or $P307_{SQ-8C}$ for 2 h at 22-25°C in 100% plasma or indicated concentrations of chloride salts of sodium, calcium and magnesium and human serum albumin in 50 mM Tris-HCl, pH 7.5. Serial dilutions were plated for cfu counting. The error bars show standard deviation and the black horizontal lines mark the limit of detection for cfu/mL.

Figure 4.4 *In vivo* activity of $P307_{SQ-8C}$ versus that of polymyxin B on tape-stripped mice infected with *A. baumannii* strain #1791.

Topical treatments included no treatment (negative control), 2 μg polymyxin B (1.5 nmol) and 200 μg $P307_{SQ-8C}$ (46.5 nmol) for 2 h. The bars show the mean values and each dot represents one mouse. Statistically significant differences were noted for the comparison pairs: negative control and polymyxin B ($P = 0.0148$) and negative control and $P307_{SQ-8C}$ ($P = 0.0157$), with ~2-log-drop in *A. baumannii* by each treatment (Ordinary one-way ANOVA, Multiple comparisons, Uncorrected Fisher's LSD test). The dotted line marks the limit of detection.

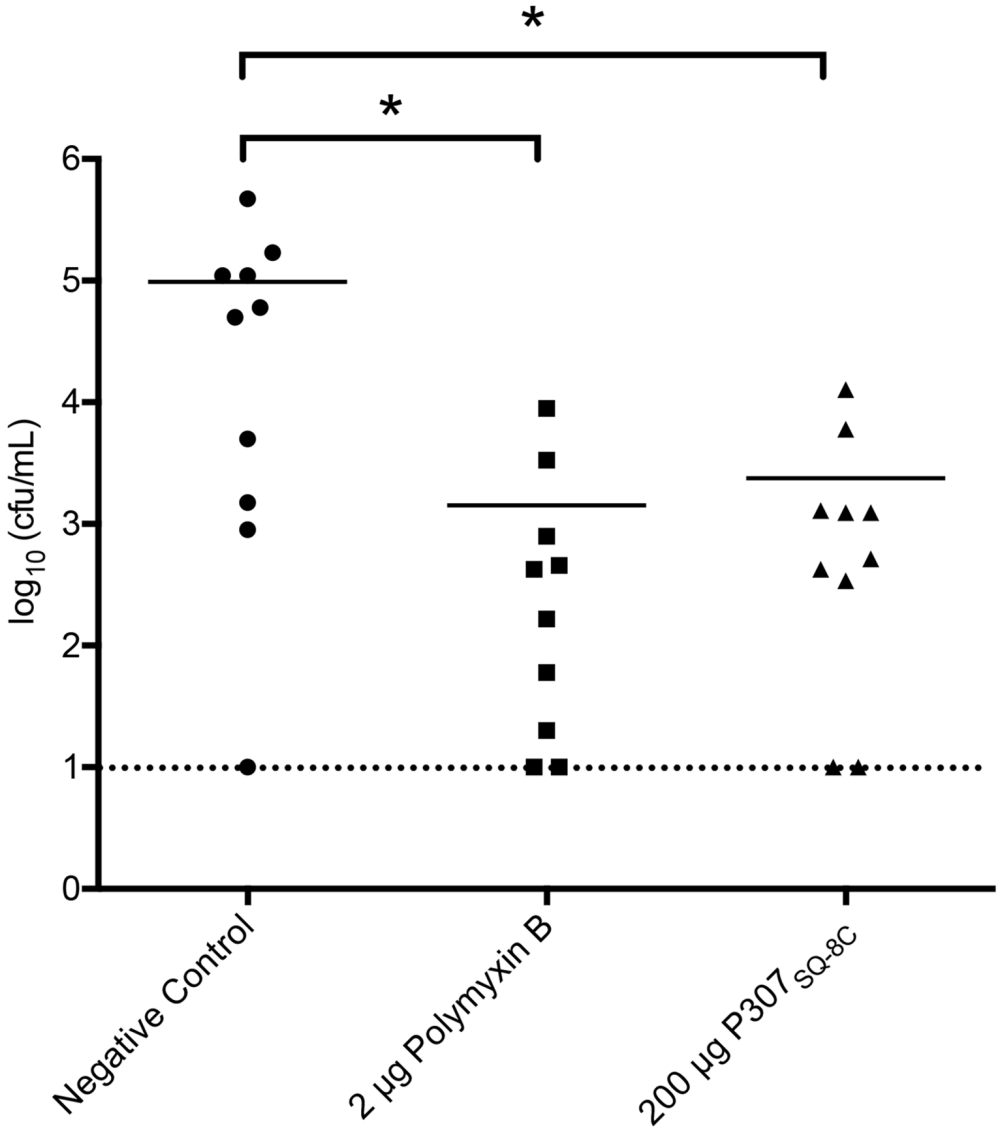
*
*
6
5
4
3
2
1
0
log10 (cfu/mL)
Negative Control
2 µg Polymyxin B
200 µg P307 SQ-8C

4.3 ACKNOWLEDGMENTS

I would like to thank Clara A. Eastby and Dr. Chad W. Euler for B cell cultures and Mary Windels for scheduling hospital appointments for blood collection. Dr. Euler also provided invaluable guidance and assistance with animal experiments. I thank Gabriella Balaa for her excellent assistance with plasma experiments. I am also grateful to Rockefeller University Hospital as well as Comparative Bioscience Center (CBC).

Chapter 2, 3 and 4 are based on a published article co-authored (in order) by: Dr. Rolf Lood, Benjamin Y. Winer, Douglas R. Deutsch, Dr. Chad W. Euler and Dr. Vincent A. Fischetti. The study was supported by a grant from Contrafect Corporation. We thank Michael Wittekind and Raymond Schuch for useful discussions and suggestions during the course of these studies.

5 CHAPTER 5 – DISCUSSION

5.1 Lysin-based antimicrobial peptides

5.1.1 Sequence and structure

The antimicrobial peptides in this study (Table 2.1) were designed by observing the 'activity-contributing' parts of phage lysins PlyF307 (47) and LysAB2 (46) and an antimicrobial peptide HBc ARD (52). PlyF307 was found to be the most active among the 21 distinct lysins isolated by screening a genomic library of prophages that were induced from 13 *A. baumannii* strains. Instead of the domain structures typical of lysins, PlyF307 comprises a single lysozyme domain and a C-terminus that has unusually high positive net charge (+7). The amino acids 108-138 of PlyF307 are also 41.2% similar and 17.6% identical to the amino acids 113-145 of LysAB2. In LysAB2, those amino acids are essential and their deletion leads to 40% activity loss although they do not encompass the active site of the enzyme. Considering the high activity of PlyF307, we synthesized the 31 amino acids of PlyF307 as peptide P307 to investigate its stand-alone bactericidal activity. In HBc ARD, the removal of the last 8 amino acids (SQSRESQC) diminishes its activity against *S. aureus*. In the hope of enhancing P307 activity, $P307_{SQ\text{-}8C}$ was designed by piecing together P307 and SQSRESQC. Lastly, $P307_{AE\text{-}8}$ was constructed to compare the original extension AEMELFLK of PlyF307 to $P307_{SQ\text{-}8C}$ extension.

The structural predictions (58-60) of PlyF307 and $P307_{SQ\text{-}8C}$ revealed double parallel helices joined by a loop for both $P307_{AE\text{-}8}$ and $P307_{SQ\text{-}8C}$. P307 was just a turn and a half shorter. And the helices were amphipathic in nature according to the helical wheel plot (61) (Figure 2.2). However, when the activities were compared, P307 and $P307_{AE\text{-}8}$ had similar activities while $P307_{SQ\text{-}8C}$ with its polar amino acids showed the

highest bactericidal activity of all (Figure 2.3A). The addition of P307 and SQ-8C extension separately did not achieve the same result as $P307_{SQ-8C}$ (Figure 2.3B) and the extension by itself was inert. But scrambling the sequence to CSQRQSES in $P307_{CS-8}$ did not affect the bactericidal activity (Figure 2.3C). Although we tested only 1 out of 40,320 permutations, comparable killing activities by $P307_{SQ-8C}$ and $P307_{CS-8}$ did suggest that the 8 amino acids could be arranged in an alternate order.

5.1.2 *In vitro* activity

The *in vitro* activity assays of P307 and $P307_{SQ-8C}$ were conducted with clinical isolates to examine their antibacterial potential. Bactericidal assays showed that the peptides are more active at higher pH (Figure 2.4A) and that $P307_{SQ-8C}$ acted faster than P307, easily achieving >6-log-kill in 90 min (Figure 2.4D). They were specific to *A. baumannii* with slight activities against *B. anthracis*, *S. aureus* and *P. aeruginosa* and no activity against *E. coli* or *K. pneumoniae* at pH 7.5 (Figure 2.5). This selectivity towards *A. baumannii* at pH 7.5 suggests that the outer layers of *A. baumannii* are more negatively charged than those of the other bacterial species included in the assay since at pH 8.8, the selectivity is nullified. They were also capable of killing biofilm-associated *A. baumannii* albeit requiring higher concentrations (Figure 2.6B). However, their MICs were much higher than that of polymyxin B (Table 2.2). It is possibly due to the interference of cations in the growth media. More experimental data are required to determine their susceptibility breakpoints, e.g. pharmacokinetics and pharmacodynamics (72). Nevertheless, $P307_{SQ-8C}$ could be put to use for decontamination in clinical settings because of its fast acting and biofilm killing properties. Since medical equipment and furniture are important hospital reservoirs of *A. baumannii* (15, 16), $P307_{SQ-8C}$ could be

used on these surfaces for quick bacterial removal. Moreover, catheter- and ventilator-associated diseases are caused by the persistence of *A. baumannii* as biofilms (73), they could be prevented by lining the surfaces with $P307_{SQ-8C}$.

5.2 Mechanism of action

Biochemical characterizations of peptides-bacteria interactions have indicated the target site to be the outer and inner membranes of *A. baumannii*. Higher pH in Tris buffer elicited better killing activities of the peptides while higher salt concentrations lessened their effectiveness (Figure 2.4A and B). Since Tris is a chemical substance known to permeabilize membranes (74), it is not surprising that the peptides' activities were higher in Tris buffer than in phosphate buffer. However, it is notable that higher pH and fewer cations promote killing. Even *E. coli* and *K. pneumoniae* that were resistant to the peptides at pH 7.5 became susceptible to killing at pH 8.8 (Figure 3.2). Since the theoretical isoelectric points of P307 and $P307_{SQ-8C}$ are 10.70 and 10.38, respectively, their net charges should not alter at pH 7.5 and pH 8.8. Possibly the changes occur on the bacterial membranes. In Gram-negative bacteria, the outer leaflet of the outer membrane, being largely composed of polyanionic LPS, is stabilized by divalent cations (Ca^{2+} and Mg^{2+}) (75). At higher pH and lower salt concentrations, the positively charged peptides could more easily establish ionic interactions with the outer membrane to permeate the membranes and induce killing.

Further evidence by synergy, TEM and SYTOX green uptake assays also supported the membrane permeabilization as the peptides' mechanism of action. First, the peptides exhibited *in vitro* synergy with polymyxin B whose membrane target is lipid A of LPS (71). Among different possible mechanisms of synergy (76), the most likely

scenario is the complementary actions from having the same target, i.e. both the polymyxin B and the peptides killed the bacteria by permeabilizing the membrane in a way that enhanced each other's activity. The lack of synergy with levofloxacin and ceftazidime suggested that DNA and cell wall were not the targets of the peptides. Indeed, the DNA-binding assay showed that P307 did not bind to DNA (Figure 3.3). Next, TEM images of *A. baumannii* treated with $P307_{SQ-8C}$ showed mostly intact bacterial 'ghosts' with altered cytoplasmic content (Figure 3.4B and C) as if the cytoplasm had leaked out of the bacteria through the tiny holes punched by the peptide. In contrast, more bacterial debris was formed by lysozyme that targets the peptidoglycan (Figure 3.4D). During $P307_{SQ-8C}$ killing, the permeabilization of the inner membrane seemed to be the limiting step because combined treatment with $P307_{SQ-8C}$ and lysozyme resulted in more extensive debris formation. The outer membrane disruption of $P307_{SQ-8C}$ provided the lysozyme access to the peptidoglycan and the lysozyme action preceded the inner membrane disruption of $P307_{SQ-8C}$. Lastly, the results from SYTOX green uptake assay (Figure 3.5) confirmed that both outer and inner membranes were compromised by the peptides to allow the inflow of SYTOX green dye.

However, the ability of the peptides to permeabilize bacterial membranes raises the question of how their parent phage lysin PlyF307 is regulated by the phage during the lytic cycle. The regulation of phage lysin is necessary to prevent pre-mature lysis of bacteria before the production of phage progeny. Thus, there must be mechanisms in place to prevent the positively charged region of PlyF307 disrupting the cytoplasmic membrane from within the cell before the progeny are assembled. The peptide region might be inhibited by structural conformation or temporal regulation or the non-optimal

pH and salt conditions of the cellular environment. Future experiments with the phage from which PlyF307 was isolated are necessary to clarify the regulation of PlyF307.

5.3 *In vivo* activity

The safety and efficacy of the peptides were investigated by hemolysis, cytotoxicity, limulus amebocyte lysate (LAL) and plasma interference assays. First, the hemolysis and B cell toxicity assays showed that the peptides did not lyse human red blood cells and B cells. Although the peptides killed the bacteria by permeabilizing the membranes, the mammalian membranes were spared. The cells remained viable at ~500 μg/mL of $P307_{SQ-8C}$ (Figure 4.1). Next, the LAL assay showed that the peptides released endotoxins upon killing the bacteria. The amount released by $P307_{SQ-8C}$ was ~40 times higher than that by polymyxin B (Figure 4.2) since the latter binds to lipid A and lowers the level of detection. The released endotoxins could potentially initiate undesirable inflammatory responses. Lastly, the bactericidal assay in plasma showed that the killing activities of the peptides were interfered by plasma and its components such as monovalent and divalent cations and serum albumin. The endotoxin release and plasma interference together indicated that prophylactic use might not be feasible. Thus, mouse skin infection model was selected to investigate the *in vivo* activity of $P307_{SQ-8C}$. Using 200 μg of $P307_{SQ-8C}$ in distilled water, *A. baumannii* bacterial load on the irritated skin surface was significantly reduced (~2-log-drop) (Figure 4.4), indicating that $P307_{SQ-8C}$ could be used in topical applications.

5.4 Opportunities for improvement

Resistance development was not observed when selecting from 10^5 cfu/mL. Due to material limitations, resistance evolutions at low frequency were not detected.

Alternative experiments need to be conducted to better understand the potential of *A. baumannii* developing resistance. For example, the MICs for colistin-resistant clones should be determined and compared with non-resistant clones since colistin also permeabilizes the membranes to kill the bacteria. Another option is to mutagenize *A. baumannii* and screen for resistant clones.

Moreover, there are rooms for further development to achieve higher *in vivo* activities even though the peptides are highly effective at killing *A. baumannii in vitro*. Since disulfide bond formation contributes to the high activity of $P307_{SQ\text{-}8C}$ (Figure 3.1) and only ~5-10% of the molecules are dimers, $P307_{SQ\text{-}8C}$ that forms permanent dimers (e.g. with C-C bond in place of S-S bond between cysteines) might be designed by incorporating unnatural amino acids. By changing the S-S bond to C-C bond, the importance of disulfide bond formation versus that of dimer formation can also be differentiated. For example, taking advantage of the peptides' preference for high pH, alkaline excipients can be used to achieve higher killing effect. However, a fine balance needs to be maintained for high activity versus alkaline toxicity. Moreover, peptides can be further engineered to be active in plasma. By using x-ray crystallography or NMR, residues that interact with serum albumin can be deciphered and altered to minimize the amount of peptides binding to the most abundant protein in plasma. The challenge in this case is to achieve the goal without compromising the activity. Other strategies to improve bioavailability include fusing $P307_{SQ\text{-}8C}$ to an antibody F_C fragment (77) and creating 'structurally nanoengineered antimicrobial peptide polymers' (SNAPPs) (78) with $P307_{SQ\text{-}8C}$. By increasing the effective size of the peptide by F_C fusion, the adsorption to serum albumin could be reduced and F_C fragment tag can also be recognized by F_C

receptors on immune cells. The bulkiness, however, can sterically interfere with the peptide's traversing the outer membrane to destabilize the inner membrane. Last, but not least, SNAPPs are star-shaped polymers with multi-functional initiator poly(amidoamine) PAMAM core that has 16 or 32 primary amines onto which antimicrobial peptides (AMPs) are attached. The original version of SNAPPs with AMPs made up of poly lysine and valine killed Gram-negative bacteria indiscriminately and had slight cytotoxic effects at high concentrations. The efficacy was retained in the presence of serum despite aggregate formation (78). Creating SNAPPs with $P307_{SQ\text{-}8C}$ can potentially increase the *in vivo* activity of $P307_{SQ\text{-}8C}$ by effectively increasing the local concentrations 16 to 32 folds. In contrast to the original SNAPPs, $P307_{SQ\text{-}8C}$ SNAPPs might be more specific to *A. baumannii* and less toxic to mammalian cells.

5.5 Potential practical uses

The pH dependence and salt intolerance might prevent broad *in vivo* application but skin infections could be treated topically with the peptides. In addition, they could be used in hospitals to decontaminate abiotic surfaces and eliminate reservoirs to prevent future outbreaks as mentioned above.

6 CHAPTER 6 – CONCLUSION

Due to the notable antibiotic resistance mechanisms of *A. baumannii* (29), membrane-acting drugs like polymyxin B and colistin, with toxic side effects and rising resistance, are now the last resort drugs (27). To address the *A. baumannii* threat, several groups have evaluated the use of bacteriophage endolysins to kill multidrug-resistant *A. baumannii* (42, 46, 47). It has been hypothesized that the innate bactericidal activities of some of these lysins stem from the permeabilization of the bacterial outer membrane by the highly positively charged C-terminal portions (46, 47). In this study, we showed that P307, a C-terminal-based peptide from PlyF307 (47), by itself, had high *in vitro* bactericidal activity (Figure 2.3A). Furthermore, we demonstrated that P307 could be further engineered for log-fold increased activity. Compared to P307, or $P307_{AE\text{-}8}$ with the eight amino acids (AEMELFLK) constituting the full C-terminal part of native PlyF307 (Table 2.1), the modified peptide $P307_{SQ\text{-}8C}$ with polar amino acids (SQSRESQC) at the C-terminus was 10-15 times more active (Figure 2.5 and Table 2.2). Comparison of $P307_{SQ\text{-}8C}$ to the scrambled $P307_{CS\text{-}8}$ revealed that the 6 neutral and 2 charged polar amino acids (SQSRESQC) could be added in an alternate order for similar activity (Figure 2.3C). Thus, while both AEMELFLK and SQSRESQC complete the length of the alpha helix to correspond to the adjacent helix in the hairpin structure (Figure 2.2), it is the characteristics of the amino acids in the SQSRESQC sequence (not the structure) that dictate the increase in activity.

Both P307 and $P307_{SQ\text{-}8C}$ displayed high *in vitro* bactericidal activities. Not only were they effective against numerous clinical isolates of *A. baumannii* (Figure 2.5) but they also killed bacteria in biofilms on the surface of catheters (Figure 2.6B). Since the

success of *A. baumannii* as an opportunistic pathogen is attributed to its improved survival through biofilm formation and persistence in hospital environments (79), the ability of the peptides to kill biofilm-associated bacteria could be harnessed to disinfect hospital environments as well as to eliminate *A. baumannii* from the lumens of catheters *in situ*. While the *in vivo* utility of the peptides might be limited due to the diminished activity in plasma, the peptides could still be useful on abiotic surfaces such as coatings for ventilators and catheters.

To further increase the potency of the peptides, we analyzed the mechanism of action by various *in vitro* characterizations. The peptides were more active in higher pH but did not tolerate salinity. *E. coli* and *K. pneumoniae* were resistant to the peptides at pH 7.5 but were susceptible at pH 8.8 (Figure 2.5 and 3.2). Since the charges on the peptide were not expected to vary as the pH changed from 7.5 to 8.8, we reasoned that the changes likely occurred on the bacterial membrane. At higher pH, the bacterial membrane can lose its cations, allowing the positively charged peptides to establish ionic interactions to disrupt the membrane integrity. Based on these observations and data, we postulate the following mechanism of action (Figure 6.1): $P307_{SQ\text{-}8C}$ establishes ionic interactions with the bacterial outer and inner membranes, traversing the peptidoglycan with its small size (4.3 kDa). In the process, the peptide disrupts both membranes (as suggested by endotoxin release assay and shown by TEM images and SYTOX® Green uptake assay) killing the cell. Assay with TCEP and $P307_{SQ\text{-}8A}$ also suggested that the bactericidal activity was higher (by ~2-logs) when $P307_{SQ\text{-}8C}$ was dimerized. With this knowledge base, we are currently exploring additional engineering strategies to further improve both PlyF307 and $P307_{SQ\text{-}8C}$.

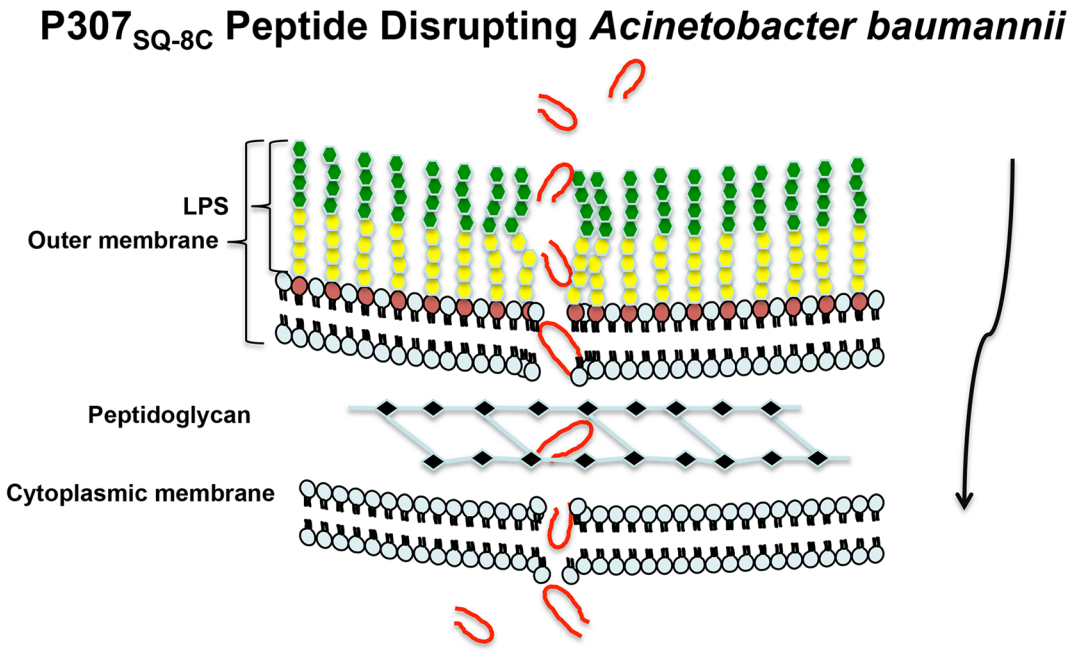

Figure 6.1 Proposed mechanisms of action.

When added externally the positively charged peptide $P307_{SQ-8C}$ disrupts the outer membrane and traverses the peptidoglycan because of its small size. The peptide will then disrupt the cytoplasmic membrane, resulting in hypotonic lysis and bacterial death.

Nosocomial *A. baumannii* infections of deep wounds, burns and bone or bone marrow are highly prevalent and the isolates are often multidrug resistant (17). Since one of the common infection routes of *A. baumannii* is through damaged skin, we utilized an already established skin infection model (69) for our *in vivo* characterization of $P307_{SQ-8C}$. The backs of the mice were shaved and tape-stripped to create skin irritations, which were then inoculated with 10^6 cfu of *A. baumannii* strain #1791. After 16 h of infection, mice were topically treated with a single dose of 46.5 nmol $P307_{SQ-8C}$ or 1.5 nmol polymyxin B. Both treatments significantly lowered the bacterial burden (~2-log decrease) in the skin (Figure 4.4).

In conclusion, we engineered the positively charged C-terminal peptide P307 from the *A. baumannii* phage lysin PlyF307 for improved bactericidal activity. The peptides exhibited high *in vitro* activities, and thus could potentially be utilized to control *A. baumannii* on abiotic surfaces. The target of the peptides appeared to be the bacterial membrane and the interaction likely occurred through electrostatic forces. Despite the membrane target, the peptides did not lyse or kill human red blood cells and B cells. Although body fluids and cations interfered with the activities of the peptides, $P307_{SQ-8C}$ significantly decreased the bacterial cell count in a murine skin infection by *A. baumannii*. We are currently investigating different designs to improve the activities of the peptides as well as other phage lysins against *A. baumannii*.

6.1 ACKNOWLEDGMENTS

This chapter is based on a published article co-authored (in order) by: Dr. Rolf Lood, Benjamin Y. Winer, Douglas R. Deutsch, Chad W. Euler and Dr. Vincent A. Fischetti. I am grateful to Dr. Fischetti for creating the model figure for MOA.

7 APPENDIX

7.1 Interesting observations

7.1.1 Anaerobic environment decreased bactericidal activities of P307 and $P307_{SQ-8C}$

While investigating the peptides' mechanisms of action, bactericidal experiments were conducted in an anaerobic chamber to investigate the effect of oxygen. *A. baumannii* strain #1791 was washed with and re-suspended in 50 mM Tris-HCl (pH 7.5 or pH 8.8) and treated with 50 or 200 μg/mL of P307 or $P307_{SQ-8C}$ at 37°C for 2 h aerobically or anaerobically. Then the bacteria were serially diluted and plated on TSB agar in respective oxygen environments. Afterwards the plates were incubated aerobically since *A. baumannii* is strictly aerobic.

The bacteria became insensitive to the peptides at pH 7.5 and increasing the pH to 8.8 restored the sensitivities (Figure 7.1). The experiments were conducted twice in triplicate. These results indicated that oxygen is necessary at lower pH to kill the bacteria while at high pH, ionic interactions between peptides and membranes are strong enough to kill the bacteria by disrupting the membranes without the need for oxygen. The oxygen requirement at lower pH is interesting because it has been previously argued that bacterial cell death by bactericidal antibiotics induced reactive oxygen species (ROS) (80, 81) and apoptotic pathway (82). Refuting these arguments, other research groups stated that bacterial cell death induced by antibiotics does not depend on ROS formation, ROS being the by-product of stress response (83, 84). Peptides requiring oxygen for bactericidal effect seems to suggest the involvement of reactive oxygen species. However, oxygen-dependent transport of the peptide across the outer membrane cannot be completely ruled out. Using luminol and terephthalate has not been successful at

detecting the ROS formation. Therefore, more experimental data are required to resolve the issue. For example, ROS sensitive fluorescent dye, DCFDA (2',7'-dichlorofluorescin diacetate) could be used for better ROS detection.

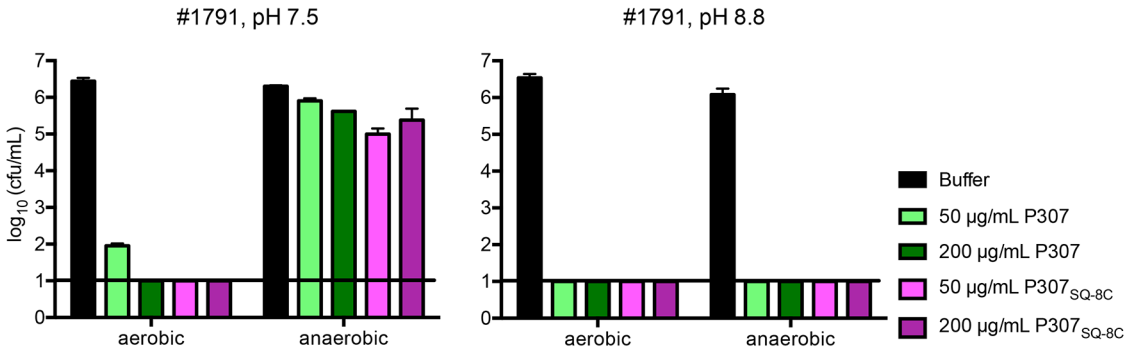

Figure 7.1 Bactericidal activities of the peptides in aerobic versus anaerobic conditions.

A. baumannii strain #1791 was treated with 50 or 200 µg/mL P307 or $P307_{SQ-8C}$ for 2 h at 37°C in 50 mM Tris-HCl (pH 7.5 or 8.8) under aerobic or anaerobic conditions. Serial dilutions were plated for cfu counting. The error bars show standard deviation and the black horizontal lines mark the limit of detection.

7.1.2 ATCC 17978 caused clearings on agar overlay containing DH5α

The surrounding area of *A. baumannii* strain ATCC 17978 colony was clear on an agar overlay of *E. coli* strain DH5α (Figure 7.2). The clearing could be induced by ATCC 17978 killing DH5α and the potential killing agents are phages, Type VI secretion system and phage lysins.

Although most phages are strain specific, there also exist polyvalent phages that infect more than one genus (85). The possibility was examined by plaque forming assay. The prophages from ATCC 17978 were induced with mitomycin C and concentrated with PEG-8000. The phage preparation was spotted on an agar overlay of DH5α, but no plaque was observed. Most likely, phages were not involved in the killing.

A. baumannii has been shown to use type VI secretion system (T6SS) for bacterial competition (86). This possibility has not been thoroughly examined but ATCC 17978 indeed possessed T6SS in its genome and deleting the essential components could reveal whether T6SS is used for DH5α killing.

Last, but not least, phage lysins of Gram-negative bacteria have been shown to perform non-phage related functions. For example, in *Salmonella* phage lysins are retained from past infections and become orphan phage enzymes as indicated by the difference in DNA composition in the up and downstream of the gene (87). They are utilized by the bacterium for infection (88), toxin secretion (89) and virulence (87). Such uses of phage lysins by *A. baumannii* have not been reported before. However, *A. baumannii* strains are usually poly-lysogenic and some of the prophages are no longer intact. According to PHAge Search Tool (PHAST) analysis (90), ATCC 17978 possessed three prophages, two of which are intact and the third questionable. To investigate

whether the lysins are used to kill DH5α, we are investigating the RNA expression level of the three lysins in ATCC 17978.

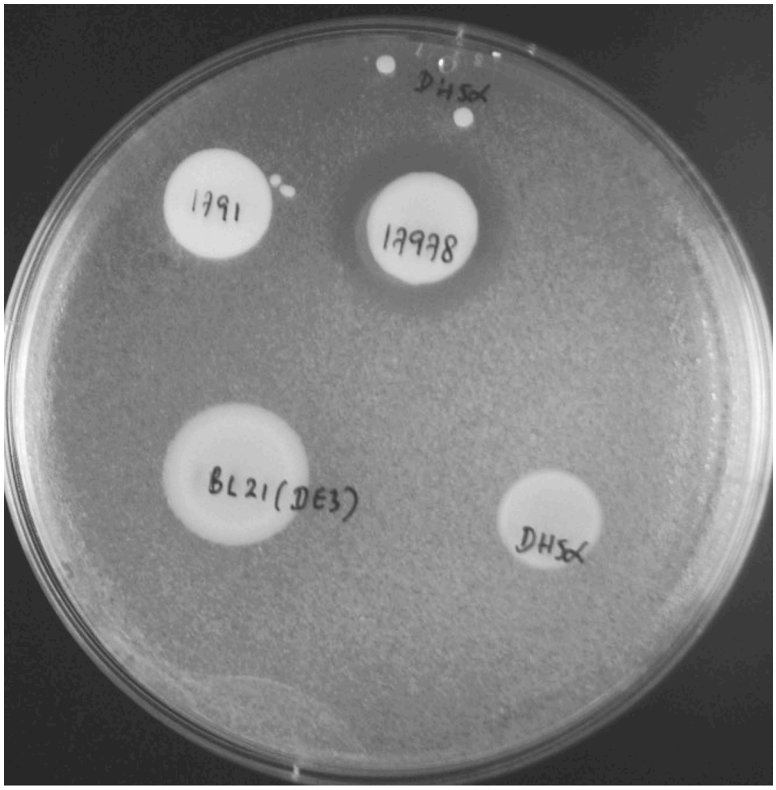

Figure 7.2 Clearing zone around *A. baumannii* ATCC 17978 colony on *E. coli* DH5α agar overlay.

7.2 PlyF309

7.2.1 BACKGROUND

PlyF309 (GenBank Accession Number KJ740397.1) is the second most active among the 21 distinct lysins isolated from a genomic library of prophages inside 13 *A. baumannii* strains (47). According to a National Center for Biotechnology Information Basic Local Alignment Search Tool (BLAST) search, it is composed of an N-terminal catalytic domain (glycosyl hydrolase family 108) and a C-terminal cell-wall binding domain (peptidoglycan binding 3) (Figure 7.1). The molecular weight of PlyF309 is ~21 kDa and the isoelectric point is 8.40. The lysin was purified and its *in vitro* bactericidal activities were analyzed.

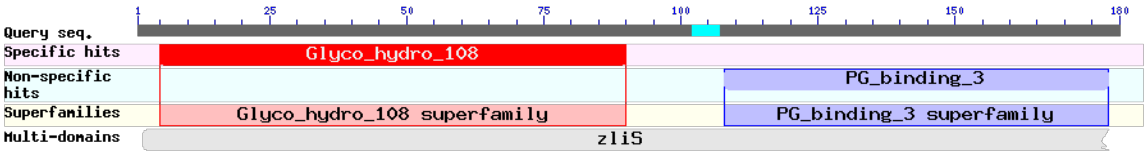

Figure 7.3 Domain organization of PlyF309.

7.2.2 MATERIALS AND METHODS

7.2.2.1 Expression and purification

Overnight culture of *E. coli* DH5α with the pBAD24-PlyF309 construct was diluted 1:100 in LB containing 100 µg/ml ampicillin and was incubated at 37°C, with shaking at 200 rpm, until reaching an optical density at 600 nm (OD_{600}) of 0.5. The expression of PlyF309 was induced by the addition of 0.2% arabinose, and expression continued overnight at 30°C. The cells were collected, resuspending in 50 mM sodium phosphate (pH 6.8), and homogenized using an Emulsiflex-C5 homogenizer (Avestin). The cellular debris was removed by centrifugation (16,000 × *g* for 45 min at 4°C) followed by sterile filtration (0.22 µm) to generate a crude lysate. The crude lysate of

PlyF309 in 50 mM sodium phosphate (pH 6.8) was applied to a HiTrap SP FF column (GE Healthcare Life Sciences, Uppsala, Sweden) using the Äkta fast protein liquid chromatography (FPLC) system (GE Healthcare Life Sciences), and fractions were eluted with a linear gradient of 2 M NaCl. Peaks of interest were pooled and BCA assay was used to determine the concentration.

7.2.2.2 *In vitro* bactericidal assays

PlyF309 was biochemically characterized to understand the effects on its *in vitro* bactericidal activity by pH, monovalent cation Na^+, divalent cations (Ca^{2+} and Mg^{2+}), chelating agent EDTA and growth phases (log and stationary). For these assays, *A. baumannii* strain #1791 was washed and re-suspended in respective buffer at OD_{595}~1.0 (>10^8 cfu/mL) and 250 μg/mL of PlyF309 was used. The strain specificity of PlyF309 was investigated with 15 *A. baumannii* strains #1775-1777 and #1788-#1799 using 250 μg/mL PlyF309, 250 μM EDTA and 37.5 mM Tris buffer (pH 8.0). The experiments were conducted at least in duplicate.

7.2.3 RESULTS

7.2.3.1 *In vitro* characterization

PlyF309 was most active in high pH (8.0 and 8.8) and was not tolerant to monovalent or divalent cations. The higher the EDTA concentrations, the more active PlyF309. The stationary phase bacteria are the most sensitive among the growth phases and PlyF309 showed higher activities against strains #1775, #1776, #1777, #1788, #1790, #1791, #1795, #1798 and #1799 than the rest of the 6 strains (Table 7.1).

Table 7.1 Summary of PlyF309 activities in different assay conditions

Assay condition	Percent killing
Sodium acetate buffer (pH 5.2)	56.25
Tris-HCl buffer (pH 6.07)	78.57
Tris-HCl buffer (pH 6.8)	60.87
Tris-HCl buffer (pH 8.0)	94.44
Tris-HCl buffer (pH 8.8)	87.50
75 mM NaCl	0
150 mM NaCl	14.29
5 mM $CaCl_2$	0
5 mM $MgCl_2$	0
0.1 mM EDTA	58.33
0.25 mM EDTA	68.18
0.5 mM EDTA	84.25
Early log phase 2 h	15.38
Log phase 4 h	15.38
Late log phase 8 h	35.29
Stationary phase 32 h	50.00
#1775	82.65
#1776	86.80
#1777	66.39
#1788	76.92
#1789	0
#1790	71.43
#1791	75.00
#1792	6.25
#1793	0
#1794	0
#1795	72.73
#1796	0
#1797	16.67
#1798	66
#1799	89.50

7.2.4 DISCUSSION

The theoretical isoelectric points of PlyF309 catalytic and binding domains are 5.01 and 9.56, respectively, which means that the catalytic domain is negatively charged and the binding domain is positively charged in the buffers tested. Better killing activities were achieved with high pH and high EDTA concentrations whereas the cations diminished the activities, indicating that the outer membrane barrier did impede PlyF309 from getting access to the peptidoglycan. It is also intriguing that PlyF309 showed growth phase and strain preferences. PlyF309 was also much less active than PlyF307. However, these results are likely due to the use of higher number of bacteria (10^8 vs 10^6 cfu/mL used for PlyF307 assays) while the concentration of the PlyF309 was only 2.5 times higher (250 μg/mL vs 100 μg/mL used for PlyF307 assays).

7.2.5 ACKNOWLEDGMENTS

I am grateful to Dr. Rolf Lood and Benjamin Y. Winer for their guidance and assistance.

8 REFERENCES

1. **Perez F**, **Hujer AM**, **Hujer KM**, **Decker BK**, **Rather PN**, **Bonomo RA**. 2007. Global challenge of multidrug-resistant *Acinetobacter baumannii*. Antimicrob Agents Chemother **51**:3471–3484.

2. **Potron A**, **Poirel L**, **Nordmann P**. 2015. Emerging broad-spectrum resistance in *Pseudomonas aeruginosa* and *Acinetobacter baumannii*: Mechanisms and epidemiology. Int J Antimicrob Agents **45**:568–585.

3. **Fishbain J**, **Peleg AY**. 2010. Treatment of *Acinetobacter* infections. Clin Infect Dis **51**:79–84.

4. **Dijkshoorn L**, **Nemec A**. 2008. The Diversity of the genus *Acinetobacter*. *In* Gerischer, U (ed.), Acinetobacter Molecular Biology. Caister Academic Press.

5. **Doughari HJ**, **Ndakidemi PA**, **Human IS**, **Benade S**. 2011. The ecology, biology and pathogenesis of *Acinetobacter* spp.: An overview. Microbes Environ **26**:101–112.

6. **Gonzalez-Villoria AM**, **Valverde-Garduno V**. 2016. Antibiotic-resistant *Acinetobacter baumannii* increasing success remains a challenge as a nosocomial pathogen. Journal of Pathogens.

7. **Almasaudi SB**. 2016. *Acinetobacter* spp. as nosocomial pathogens: Epidemiology and resistance features. Saudi Journal of Biological Sciences.

8. **European Centre for Disease Prevention and Control**. 2016. Carbapenem-resistant *Acinetobacter baumannii* in healthcare settings. *In*. Stockholm: ECDC.

9. **Stirland RM**, **Hillier VF**, **Steyger MG**. 1969. Analysis of hospital bacteriological data. J clin Path suppl (Coll Path) **3**:82–86.

10. **Morohoshi T**, **Saito T**. 1977. β-lactamase and β-lactam antibiotics resistance in *Acinetobacter anitratum* (syn.: *A. calcoaceticus*). J Antibiot **30**:969–973.

11. **Beck-Sagué CM**, **Jarvis WR**, **Brook JH**, **Culver DH**, **Potts A**, **Gay E**, **Shotts BW**, **Hill B**, **Anderson RL**, **Weinstein MP**. 1990. Epidemic bacteremia due to *Acinetobacter baumannii* in five intensive care units. Am J Epidemiol **132**:723–733.

12. **Boucher HW**, **Talbot GH**, **Bradley JS**, **Edwards JE**, **Gilbert D**, **Rice LB**, **Scheld M**, **Spellberg B**, **Bartlett J**. 2009. Bad bugs, no drugs: no ESKAPE! An update from the Infectious Diseases Society of America. Clin Infect Dis **48**:1–12.

13. **World Health Organization WHO**. 2017. Global priority list of antibiotic-resistant bacteria to guide research, discovery, and development of new antibiotics.

14. **Peleg AY**, **Seifert H**, **Paterson DL**. 2008. *Acinetobacter baumannii*: Emergence of a successful pathogen. Clin Microbiol Rev **21**:538–582.

15. **Beggs CB**, **Kerr KG**, **Snelling AM**. 2006. *Acinetobacter* spp. and the clinical environment. Indoor and Built Environ **15**:19–24.

16. **Jawad A**, **Seifert H**, **Snelling AM**, **Heritage J**, **Hawkey PM**. 1998. Survival of *Acinetobacter baumannii* on dry surfaces: Comparison of outbreak and sporadic isolates. J Clin Microbiol **36**:1938–1941.

17. **Dijkshoorn L**, **Nemec A**, **Seifert H**. 2007. An increasing threat in hospitals: Multidrug-resistant *Acinetobacter baumannii*. Nat Rev Microbiol **5**:939–951.

18. **Centers for Disease Control and Prevention (CDC)**. 2013. Antibiotic resistance threats in the United States, 2013.

19. **Choi CH**, **Lee JS**, **Lee YC**, **Park TI**, **Lee JC**. 2008. *Acinetobacter baumannii* invades epithelial cells and outer membrane protein A mediates interactions with epithelial cells. BMC Microbiol **8**.

20. **Choi CH**, **Hyun SH**, **Lee JY**, **Lee JS**, **Lee YS**, **Kim SA**, **Chae JP**, **Yoo SM**, **Lee JC**. 2008. *Acinetobacter baumannii* outer membrane protein A targets the nucleus and induces cytotoxicity. Cell Microbiol, 2nd ed. **10**:309–319.

21. **Jin JS**, **Kwon S-O**, **Moon DC**, **Gurung M**, **Lee JH**, **Kim Il S**, **Lee JC**. 2011. *Acinetobacter baumannii* secretes cytotoxic outer membrane protein A via outer membrane vesicles. PLoS ONE **6**:e17027.

22. **Moon DC**, **Choi CH**, **Lee JH**, **Choi C-W**, **Kim H-Y**, **Park JS**, **Kim Il S**, **Lee JC**. 2012. *Acinetobacter baumannii* outer membrane protein A modulates the biogenesis of outer membrane vesicles. J Microbiol **50**:155–160.

23. **Johnson TL**, **Waack U**, **Smith S**, **Mobley H**, **Sandkvist M**. 2015. *Acinetobacter baumannii* is dependent on the type II secretion system and its substrate lipA for lipid utilization and *in vivo* fitness. J Bacteriol **198**:711–719.

24. **Dorsey CW**, **Beglin MS**, **Actis LA**. 2003. Detection and analysis of iron uptake components expressed by *Acinetobacter baumannii* clinical isolates. J Clin Microbiol **41**:4188–4193.

25. **Lees Miller RG**, **Iwashkiw JA**, **Scott NE**, **Seper A**, **Vinogradov E**, **Schild S**, **Feldman MF**. 2013. A common pathway for O-linked protein-glycosylation and synthesis of capsule in *Acinetobacter baumannii*. Mol Microbiol **89**:816–830.

26. **Luke NR**, **Sauberan SL**, **Russo TA**, **Beanan JM**, **Olson R**, **Loehfelm TW**, **Cox AD**, **St Michael F**, **Vinogradov EV**, **Campagnari AA**. 2010. Identification and characterization of a glycosyltransferase involved in *Acinetobacter baumannii* lipopolysaccharide core biosynthesis. Infect Immun **78**:2017–2023.

27. **Doi Y**, **Murray GL**, **Peleg AY**. 2015. *Acinetobacter baumannii*: Evolution of antimicrobial resistance—Treatment options. Semin Respir Crit Care Med **36**:85–98.

28. **Ramirez MS**, **Don M**, **Merkier AK**, **Bistué AJS**, **Zorreguieta A**, **Centrón D**, **Tolmasky ME**. 2010. Naturally competent *Acinetobacter baumannii* clinical isolate as a convenient model for genetic studies. J Clin Microbiol **48**:1488–1490.

29. **Viehman JA**, **Nguyen MH**, **Doi Y**. 2014. Treatment options for carbapenem-resistant and extensively drug-resistant *Acinetobacter baumannii* infections. Drugs **74**:1315–1333.

30. **Reardon S**. 2014. Phage therapy gets revitalized. Nature.

31. **Sulakvelidze A**, **Alavidze Z**, **Morris JG**. 2001. Bacteriophage therapy. Antimicrob Agents Chemother **45**:649–659.

32. **Debarbieux L**, **Pirnay J-P**, **Verbeken G**, **De Vos D**, **Merabishvili M**, **Huys I**, **Patey O**, **Schoonjans D**, **Vaneechoutte M**, **Zizi M**, **Rohde C**. 2016. A bacteriophage journey at the European Medicines Agency. FEMS Microbiol Lett **363**:fnv225.

33. **Kingwell K**. 2015. Bacteriophage therapies re-enter clinical trials. Nat Rev Drug Discov **14**:515–516.

34. **Pelfrene E**, **Willebrand E**, **Cavaleiro Sanches A**, **Sebris Z**, **Cavaleri M**. 2016. Bacteriophage therapy: A regulatory perspective. J Antimicrob Chemother **71**:2071–2074.

35. **Pires DP**, **Cleto S**, **Sillankorva S**, **Azeredo J**, **Lu TK**. 2016. Genetically engineered phages: A review of advances over the last decade. Microbiol Mol Biol Rev **80**:523–543.

36. **Fischetti VA**, **Nelson D**, **Schuch R**. 2006. Reinventing phage therapy: Are the parts greater than the sum? Nat Biotechnol **24**:1508–1511.

37. **Gilmer DB**, **Schmitz JE**, **Euler CW**, **Fischetti VA**. 2013. Novel bacteriophage lysin with broad lytic activity protects against mixed infection by *Streptococcus pyogenes* and methicillin-resistant *Staphylococcus aureus*. Antimicrob Agents Chemother **57**:2743–2750.

38. **Nelson D**, **Schuch R**, **Chahales P**, **Zhu S**, **Fischetti VA**. 2006. PlyC: A multimeric bacteriophage lysin. PNAS **103**:10765–10770.

39. **Schuch R**, **Nelson D**, **Fischetti VA**. 2002. A bacteriolytic agent that detects and kills *Bacillus anthracis*. Nature **418**:884–889.

40. **Fischetti VA**. 2008. Bacteriophage lysins as effective antibacterials. Curr Opin

Microbiol **11**:393–400.

41. **Lim J-A**, **Shin H**, **Kang D-H**, **Ryu S**. 2012. Characterization of endolysin from a *Salmonella* Typhimurium-infecting bacteriophage SPN1S. Res Microbiol **163**:233–241.

42. **Walmagh M**, **Boczkowska B**, **Grymonprez B**, **Briers Y**, **Drulis-Kawa Z**, **Lavigne R**. 2013. Characterization of five novel endolysins from Gram-negative infecting bacteriophages. Appl Microbiol Biotechnol **97**:4369–4375.

43. **Briers Y**, **Walmagh M**, **Van Puyenbroeck V**, **Cornelissen A**, **Cenens W**, **Aertsen A**, **Oliveira H**, **Azeredo J**, **Verween G**, **Pirnay J-P**, **Miller S**, **Volckaert G**, **Lavigne R**. 2014. Engineered endolysin-based "Artilysins" to combat multidrug-resistant Gram-negative pathogens. mBio **5**:e01379–14.

44. **Lukacik P**, **Barnard TJ**, **Buchanan SK**. 2012. Using a bacteriocin structure to engineer a phage lysin that targets *Yersinia pestis*. Biochem Soc Trans **40**:1503–1506.

45. **Lukacik P**, **Barnard TJ**, **Keller PW**, **Chaturvedi KS**, **Seddiki N**, **Fairman JW**, **Noinaj N**, **Kirby TL**, **Henderson JP**, **Steven AC**, **Hinnebusch BJ**, **Buchanan SK**. 2012. Structural engineering of a phage lysin that targets gram-negative pathogens. PNAS **109**:9857–9862.

46. **Lai M-J**, **Lin N-T**, **Hu A**, **Soo P-C**, **Chen L-K**, **Chen L-H**, **Chang K-C**. 2011. Antibacterial activity of *Acinetobacter baumannii* phage ϕAB2 endolysin (LysAB2) against both Gram-positive and Gram-negative bacteria. Appl Microbiol Biotechnol **90**:529–539.

47. **Lood R**, **Winer BY**, **Pelzek AJ**, **Diez-Martinez R**, **Thandar M**, **Euler CW**, **Schuch R**, **Fischetti VA**. 2015. Novel phage lysin capable of killing the multidrug-resistant gram-negative bacterium *Acinetobacter baumannii* in a mouse bacteremia model. Antimicrob Agents Chemother **59**:1983–1991.

48. **Murphy KM**. 2011. Janeway's Immunobiology, 8 ed. Garland Science.

49. **Dürr UHN**, **Sudheendra US**, **Ramamoorthy A**. 2006. LL-37, the only human member of the cathelicidin family of antimicrobial peptides. Biochim Biophys Acta **1758**:1408–1425.

50. **Fahrner RL**, **Dieckmann T**, **Harwig SSL**, **Lehrer RI**, **Eisenberg D**, **Feigon J**. 1996. Solution structure of protegrin-1, a broad-spectrum antimicrobial peptide from porcine leukocytes. Chem Biol **3**:543–550.

51. **Song C**, **Weichbrodt C**, **Salnikov ES**, **Dynowski M**, **Forsberg BO**, **Bechinger B**, **Steinem C**, **de Groot BL**, **Zachariae U**, **Zeth K**. 2013. Crystal structure and functional mechanism of a human antimicrobial membrane channel. PNAS **110**:4586–4591.

52. **Chen H-L**, **Su P-Y**, **Chang Y-S**, **Wu S-Y**, **Liao Y-D**, **Yu H-M**, **Lauderdale T-L**, **Chang K**, **Shih C**. 2013. Identification of a novel antimicrobial peptide from human hepatitis B virus core protein arginine-rich domain (ARD). PLoS Pathog **9**:e1003425.

53. **Li J**, **Koh J-J**, **Liu S**, **Lakshminarayanan R**, **Verma CS**, **Beuerman RW**. 2017. Membrane active antimicrobial peptides: Translating mechanistic insights to design. Front Neurosci **11**:73.

54. **Andersson DI**, **Hughes D**, **Kubicek-Sutherland JZ**. 2016. Mechanisms and consequences of bacterial resistance to antimicrobial peptides. Drug Resist Updat **26**:43–57.

55. **Yele AB**, **Thawal ND**, **Sahu PK**, **Chopade BA**. 2012. Novel lytic bacteriophage AB7-IBB1 of *Acinetobacter baumannii*: Isolation, characterization and its effect on biofilm. Arch Virol **157**:1441–1450.

56. **Popova AV**, **Zhilenkov EL**, **Myakinina VP**, **Krasilnikova VM**, **Volozhantsev NV**. 2012. Isolation and characterization of wide host range lytic bacteriophage AP22 infecting *Acinetobacter baumannii*. FEMS Microbiol Lett **332**:40–46.

57. **Jin J**, **Li Z-J**, **Wang S-W**, **Wang S-M**, **Huang D-H**, **Li Y-H**, **Ma Y-Y**, **Wang J**, **Liu F**, **Chen X-D**, **Li G-X**, **Wang X-T**, **Wang Z-Q**, **Zhao G-Q**. 2012. Isolation and characterization of ZZ1, a novel lytic phage that infects *Acinetobacter baumannii* clinical isolates. BMC Microbiol **12**:156.

58. **Zhang Y**. 2008. I-TASSER server for protein 3D structure prediction. BMC Bioinformatics 2008 9:1 **9**:40.

59. **Roy A**, **Kucukural A**, **Zhang Y**. 2010. I-TASSER: A unified platform for automated protein structure and function prediction. Nat Protoc **5**:725–738.

60. **Roy A**, **Yang J**, **Zhang Y**. 2012. COFACTOR: An accurate comparative algorithm for structure-based protein function annotation. Nucleic Acids Res **40**:W471–W477.

61. **Mól AR**, **Fontes W**, **Castro MS**. 2016. NetWheels: A web application to create high quality peptide helical wheel and net projections.

62. **Gerstmans H**, **Rodríguez-Rubio L**, **Lavigne R**, **Briers Y**. 2016. From endolysins to Artilysin®s: novel enzyme-based approaches to kill drug-resistant bacteria. Biochem Soc Trans **44**:123–128.

63. **Wellings DA**, **Atherton E**. 1997. [4] Standard Fmoc protocols. Methods Enzymol **289**:44–67.

64. **Knorr R**, **Trzeciak A**, **Bannwarth W**, **Gillessen D**. 1989. New coupling reagents in peptide chemistry. Tetrahedron Lett **30**:1927–1930.

65. **CLSI**. 2012. M07-A9: Methods for dilution antimicrobial susceptibility tests for bacteria that grow aerobically; approved standard—ninth edition. Clinical and Laboratory Standards Institute, Wayne, PA.

66. **Djurkovic S**, **Loeffler JM**, **Fischetti VA**. 2005. Synergistic killing of *Streptococcus pneumoniae* with the bacteriophage lytic enzyme Cpl-1 and penicillin or gentamicin depends on the level of penicillin resistance. Antimicrob Agents Chemother **49**:1225–1228.

67. **Park CB**, **Kim HS**, **Kim SC**. 1998. Mechanism of action of the antimicrobial peptide buforin II: Buforin II kills microorganisms by penetrating the cell membrane and inhibiting cellular functions. Biochem Biophys Res Commun **244**:253–257.

68. **Saugar JM**, **Alarcón T**, **López-Hernández S**, **López-Brea M**, **Andreu D**, **Rivas L**. 2002. Activities of polymyxin B and cecropin A-,melittin peptide CA(1-8)M(1-18) against a multiresistant strain of *Acinetobacter baumannii*. Antimicrob Agents Chemother **46**:875–878.

69. **Pastagia M**, **Euler C**, **Chahales P**, **Fuentes-Duculan J**, **Krueger JG**, **Fischetti VA**. 2011. A novel chimeric lysin shows superiority to mupirocin for skin decolonization of methicillin-resistant and -sensitive *Staphylococcus aureus* strains. Antimicrob Agents Chemother **55**:738–744.

70. **J Boohaker R**, **W Lee M**, **Vishnubhotla P**, **L M Perez J**, **R Khaled A**. 2012. The use of therapeutic peptides to target and to kill cancer cells. Curr Med Chem **19**:3794–3804.

71. **Mares J**, **Kumaran S**, **Gobbo M**, **Zerbe O**. 2009. Interactions of lipopolysaccharide and polymyxin studied by NMR spectroscopy. J Biol Chem **284**:11498–11506.

72. **Turnidge J**, **Paterson DL**. 2007. Setting and revising antibacterial susceptibility breakpoints. Clin Microbiol Rev **20**:391–408.

73. **Rodríguez Baño J**, **Marti S**, **Soto S**, **Fernández Cuenca F**, **Cisneros JM**, **Pachón J**, **Pascual A**, **Martínez Martínez L**, **McQueary C**, **Actis LA**, **Vila J**. 2008. Biofilm formation in *Acinetobacter baumannii*: Associated features and clinical implications. Clin Microbiol Infect **14**:276–278.

74. **Irvin RT**, **MacAlister TJ**, **Costerton JW**. 1981. Tris(hydroxymethyl)aminomethane buffer modification of *Escherichia coli* outer membrane permeability. J Bacteriol **145**:1397–1403.

75. **Clifton LA**, **Skoda MWA**, **Le Brun AP**, **Ciesielski F**, **Kuzmenko I**, **Holt SA**, **Lakey JH**. 2015. Effect of divalent cation removal on the structure of Gram-negative bacterial outer membrane models. Langmuir **31**:404–412.

76. **Jia J**, **Zhu F**, **Ma X**, **Cao ZW**, **Li YX**, **Chen YZ**. 2009. Mechanisms of drug combinations: Interaction and network perspectives. Nat Rev Drug Discov **8**:111–128.

77. **Wen F**, **Rubin-Pitel SB**. 2009. Engineering of therapeutic proteins, pp. 153–176. *In* Park, SJ, Cochran, JR (eds.), Protein engineering and design. CRC Press.

78. **Lam SJ**, **O'Brien-Simpson NM**, **Pantarat N**, **Sulistio A**, **Wong EHH**, **Chen Y-Y**, **Lenzo JC**, **Holden JA**, **Blencowe A**, **Reynolds EC**, **Qiao GG**. 2016. Combating multidrug-resistant Gram-negative bacteria with structurally nanoengineered antimicrobial peptide polymers. Nat Microbiol **1**:16162.

79. **Roca I**, **Espinal P**, **Vila-Farrés X**, **Vila J**. 2012. The *Acinetobacter baumannii* oxymoron: Commensal hospital dweller turned pan-drug-resistant menace. Front Microbio **3**:148.

80. **Kohanski MA**, **Dwyer DJ**, **Hayete B**, **Lawrence CA**, **Collins JJ**. 2007. A common mechanism of cellular death induced by bactericidal antibiotics. Cell **130**:797–810.

81. **Sampson TR**, **Liu X**, **Schroeder MR**, **Kraft CS**, **Burd EM**, **Weiss DS**. 2012. Rapid killing of *Acinetobacter baumannii* by polymyxins is mediated by a hydroxyl radical death pathway. Antimicrob Agents Chemother **56**:5642–5649.

82. **Dwyer DJ**, **Camacho DM**, **Kohanski MA**, **Callura JM**, **Collins JJ**. 2012. Antibiotic-induced bacterial cell death exhibits physiological and biochemical hallmarks of apoptosis. Mol Cell **46**:561–572.

83. **Liu Y**, **Imlay JA**. 2013. Cell death from antibiotics without the involvement of reactive oxygen species. Science **339**:1210–1213.

84. **Keren I**, **Wu Y**, **Inocencio J**, **Mulcahy LR**, **Lewis K**. 2013. Killing by bactericidal antibiotics does not depend on reactive oxygen species. Science **339**:1213–1216.

85. **Souza KA**, **Ginoza HS**, **Haight RD**. 1972. Isolation of a polyvalent bacteriophage for *Escherichia coli*, *Klebsiella pneumoniae*, and *Aerobacter aerogenes*. J Virol **9**:851–856.

86. **Carruthers MD**, **Nicholson PA**, **Tracy EN**, **Munson RS Jr**. 2013. *Acinetobacter baumannii* utilizes a type VI secretion system for bacterial competition. PLoS ONE **8**:e59388.

87. **Michalska K**, **Brown RN**, **Li H**, **Jedrzejczak R**, **Niemann GS**, **Heffron F**, **Cort JR**, **Adkins JN**, **Babnigg G**, **Joachimiak A**. 2013. New sub-family of lysozyme-like proteins shows no catalytic activity: Crystallographic and biochemical study of STM3605 protein from *Salmonella* Typhimurium. J Struct Funct Genomics **14**:1–10.

88. **Alam MM**, **Tsai LL**, **Rollins SM**, **Sheikh A**, **Khanam F**, **Bufano MK**, **Yu Y**, **Wu-Freeman Y**, **Kalsy A**, **Sultana T**, **Sayeed MA**, **Jahan N**, **LaRocque RC**, **Harris JB**, **Leung DT**, **Brooks WA**, **Calderwood SB**, **Charles RC**, **Qadri F**, **Ryan ET**. 2013. Identification of *in vivo*-induced bacterial proteins during human infection with *Salmonella enterica* serotype Paratyphi A. Clin Vaccine Immunol **20**:712–719.

89. **Hodak H**, **Galán JE**. 2013. A *Salmonella* Typhi homologue of bacteriophage muramidases controls typhoid toxin secretion. EMBO Rep **14**:95–102.

90. **Zhou Y**, **Liang Y**, **Lynch KH**, **Dennis JJ**, **Wishart DS**. 2011. PHAST: A Fast Phage Search Tool. Nucleic Acids Res **39**:W347–W352.